

1 **Breaking antimicrobial resistance by disrupting extracytoplasmic protein 2 folding**

3
4 R. Christopher D. Furniss^{2,†}, Nikol Kadeřábková^{1,2,†}, Declan Barker², Patricia Bernal³,
5 Evgenia Maslova⁴, Amanda A.A. Antwi², Helen E. McNeil⁵, Hannah L. Pugh⁵, Laurent
6 Doretet^{2,6,7,8}, Jessica M.A. Blair⁵, Gerald Larrouy-Maumus², Ronan R. McCarthy⁴, Diego
7 Gonzalez⁹, Despoina A.I. Mavridou^{1,2,*}

8
9 ¹Department of Molecular Biosciences, University of Texas at Austin, Austin, 78712, Texas,
10 USA

11 ²MRC Centre for Molecular Bacteriology and Infection, Department of Life Sciences,
12 Imperial College London, London, SW7 2AZ, UK

13 ³Department of Microbiology, Faculty of Biology, Universidad de Sevilla, Seville, 41012,
14 Spain

15 ⁴Division of Biosciences, Department of Life Sciences, College of Health and Life Sciences,
16 Brunel University London, Uxbridge, UB8 3PH, UK

17 ⁵Institute of Microbiology and Infection, College of Medical and Dental Sciences, University
18 of Birmingham, Birmingham, B15 2TT, UK

19 ⁶Department of Bacteriology-Hygiene, Bicêtre Hospital, Assistance Publique - Hôpitaux de
20 Paris, Le Kremlin-Bicêtre, 94270, France

21 ⁷EA7361 "Structure, Dynamics, Function and Expression of Broad-spectrum β -lactamases",
22 Paris-Sud University, LabEx Lermit, Faculty of Medicine, Le Kremlin-Bicêtre, 94270,
23 France

24 ⁸French National Reference Centre for Antibiotic Resistance, Le Kremlin-Bicêtre, 94270,
25 France

26 ⁹Laboratoire de Microbiologie, Institut de Biologie, Université de Neuchâtel, Neuchâtel,
27 2000, Switzerland

28
29 *Correspondence: despoina.mavridou@austin.utexas.edu

30 [†]These authors have contributed equally to this work

31 **ABSTRACT**

32 Antimicrobial resistance in Gram-negative bacteria is one of the greatest threats to global
33 health. New antibacterial strategies are urgently needed, and the development of antibiotic
34 adjuvants that either neutralize resistance proteins or compromise the integrity of the cell
35 envelope is of ever-growing interest. Most available adjuvants are only effective against
36 specific resistance proteins. Here we demonstrate that disruption of cell envelope protein
37 homeostasis simultaneously compromises several classes of resistance determinants. In
38 particular, we find that impairing DsbA-mediated disulfide bond formation incapacitates
39 diverse β -lactamases and destabilizes mobile colistin resistance enzymes. Furthermore, we
40 show that chemical inhibition of DsbA sensitizes multidrug-resistant clinical isolates to
41 existing antibiotics and that the absence of DsbA, in combination with antibiotic treatment,
42 substantially increases the survival of *Galleria mellonella* larvae infected with multidrug-
43 resistant *Pseudomonas aeruginosa*. This work lays the foundation for the development of
44 novel antibiotic adjuvants that function as broad-acting resistance breakers.

45
46 **IMPACT STATEMENT:** Disruption of disulfide bond formation sensitizes resistant Gram-
47 negative bacteria expressing β -lactamases and mobile colistin resistance enzymes to currently
48 available antibiotics.

51 INTRODUCTION

52

53 Antimicrobial resistance (AMR) is one of the most important public health concerns of our
54 time (1). With few new antibiotics in the pharmaceutical pipeline and multidrug-resistant
55 bacterial strains continuously emerging, it is more important than ever to develop novel
56 antibacterial strategies and find alternative ways to break resistance. While the development
57 of new treatments for Gram-negative bacteria is considered critical by the WHO (2),
58 identifying novel approaches to target these organisms is particularly challenging due to their
59 unique double-membrane permeability barrier and the vast range of AMR determinants they
60 produce. For this reason, rather than targeting cytoplasmic processes, antimicrobial strategies
61 that inhibit cell-envelope components or impair the activity of resistance determinants are
62 being increasingly pursued (3-7).

63 The Gram-negative cell envelope is home to many different AMR determinants, with β -
64 lactamase enzymes currently posing a seemingly insurmountable problem. More than 6,500
65 unique enzymes capable of degrading β -lactam compounds have been identified to date
66 (Supplementary Table 1). Despite the development of more advanced β -lactam antibiotics,
67 for example the carbapenems and monobactams, resistance has continued to emerge through
68 the evolution of many broad-acting β -lactamases (8). This constant emergence of resistance
69 not only threatens β -lactams, the most commonly prescribed antibiotics worldwide (9, 10),
70 but also increases the use of last-resort agents, like the polymyxin antibiotic colistin, for the
71 treatment of multidrug-resistant infections (11). As a result, resistance to colistin is on the
72 rise, due in part to the alarming spread of novel cell-envelope colistin resistance
73 determinants. These proteins, called mobile colistin resistance (MCR) enzymes, represent the
74 only mobilizable mechanism of polymyxin resistance reported to date (12). Since their
75 discovery in 2015, ten families of MCR proteins have been identified and these enzymes are
76 quickly becoming a major threat to the longevity of colistin (13). Alongside β -lactamases and
77 MCR enzymes, Resistance-Nodulation-Division (RND) efflux pumps further enrich the
78 repertoire of AMR determinants in the cell envelope. These multi-protein assemblies span the
79 periplasm and remove many antibiotics (14, 15) rendering Gram-negative bacteria inherently
80 resistant to important antimicrobials.

81 Inhibition of AMR determinants has traditionally been achieved through the development of
82 antibiotic adjuvants. These molecules impair the function of resistance proteins and are used
83 in combination with existing antibiotics to eliminate challenging infections (4). Whilst this
84 approach has proven successful and has led to the deployment of several β -lactamase
85 inhibitors that are used clinically (4), it has so far not been able to simultaneously
86 incapacitate different classes of AMR determinants. This is because antibiotic adjuvants bind
87 to the active site of a resistance enzyme and thus are only effective against specific protein
88 families. To disrupt AMR more broadly, new strategies have to be developed that target the
89 biogenesis or stability, rather than the activity, of resistance determinants. In this way, the
90 formation of multiple resistance proteins can be inhibited at once, instead of developing
91 specific compounds that inactivate individual AMR enzymes after they are already in place.

92 In extracytoplasmic environments protein stability largely relies on the formation of disulfide
93 bonds between cysteine residues (16, 17). Notably, in the cell envelope of Gram-negative
94 bacteria this process is performed by a single pathway, the DSB system, and more
95 specifically by a single protein, the thiol oxidase DsbA (18-22). DsbA has been shown to
96 assist the folding of hundreds of proteins in the periplasm (21, 23, 24) (Figure 1A), including
97 a vast range of virulence factors (25, 26). As such, inhibition of DSB proteins has been

101 proposed as a promising broad-acting strategy to target bacterial pathogenesis without
102 impairing bacterial viability (19, 25-27). Nonetheless, the contribution of oxidative protein
103 folding to AMR has never been examined. Since several cell envelope AMR determinants
104 contain multiple cysteines (18, 28), we hypothesized that interfering with the function of
105 DsbA, would not only compromise bacterial virulence (27), but might also offer a broad
106 approach to break resistance across different mechanisms by affecting the stability of
107 resistance proteins. Here we test this hypothesis by investigating the contribution of disulfide
108 bond formation to three of the most important resistance mechanisms in the cell envelope of
109 Enterobacteria: the breakdown of β -lactam antibiotics by β -lactamases, polymyxin resistance
110 arising from the production of MCR enzymes and intrinsic resistance to multiple antibiotic
111 classes due to RND efflux pumps. We find that all these resistance mechanisms depend on
112 DsbA, albeit to a different extent, and we demonstrate that when DsbA activity is chemically
113 inhibited, resistance can be abrogated for several clinically important enzymes. Our findings
114 prove that it is possible to simultaneously incapacitate multiple classes of AMR determinants
115 and therefore are promising for the development of next-generation therapeutic approaches.

116 **RESULTS**

117
118 *The activity of multiple cell envelope resistance proteins is dependent on DsbA*
119

120 DsbA has been shown to assist the folding of numerous periplasmic and surface-exposed
121 proteins in Gram-negative bacteria (Figure 1A) (25-27). As many AMR determinants also
122 transit through the periplasm, we postulated that inactivation of the DSB system may affect
123 their folding, and therefore impair their function. To test this, we first focused on resistance
124 proteins that are present in the cell envelope and contain two or more cysteine residues, since
125 they may depend on the formation of disulfide bonds for their stability and folding (18, 28).
126 We selected a panel of twelve clinically important β -lactamases from different Ambler
127 classes (classes A, B and D), most of which are encoded on plasmids (Table 1). The chosen
128 enzymes represent different protein structures, belong to discrete phylogenetic families
129 (Supplementary Table 1) and have distinct hydrolytic activities ranging from the degradation
130 of penicillins and first, second and third generation cephalosporins (extended spectrum β -
131 lactamases, ESBLs) to the inactivation of last-resort β -lactams (carbapenemases). In addition
132 to β -lactamases, we selected five representative phosphoethanolamine transferases from
133 throughout the MCR phylogeny (Figure 1 - figure supplement 1) to gain a comprehensive
134 overview of the contribution of DsbA to the activity of these colistin-resistance determinants.
135

136 We expressed our panel of 17 discrete resistance enzymes in an *Escherichia coli* K-12 strain
137 (*E. coli* MC1000) and its isogenic *dsbA* mutant (*E. coli* MC1000 *dsbA*) and recorded
138 minimum inhibitory concentration (MIC) values for β -lactam or polymyxin antibiotics, as
139 appropriate. We found that the absence of DsbA resulted in a substantial decrease in MIC
140 values (>2-fold cutoff) for all but one of the tested β -lactamases (Figure 1B, Figure 1 - figure
141 supplement 2, Supplementary Table 2). For the β -lactamase that seemed unaffected by the
142 absence of DsbA, SHV-27, we performed the same experiment under temperature stress
143 conditions (at 43 °C rather than 37 °C). Under these conditions the lack of DsbA also resulted
144 in a noticeable drop in the cefuroxime MIC value (Figure 1 - figure supplement 3). A similar
145 effect has been described for TEM-1, whereby its disulfide bond becomes important for
146 enzyme function under stress conditions (temperature or pH stress) (29). As SHV-27 has the
147 narrowest hydrolytic spectrum out of all the enzymes tested, this result suggests that there
148 could be a correlation between the hydrolytic spectrum of the β -lactamase and its dependence
149 on DsbA for conferring resistance. In the case of colistin MICs, we did not implement a >2-
150 fold cutoff for observed decreases in MIC values as we did for strains expressing β -
151 lactamases. Polymyxin antibiotics have a very narrow therapeutic window, and there is
152 significant overlap between therapeutic and toxic plasma concentrations of colistin (30, 31).
153 Since patients that depend on colistin treatment are often severely ill, have multiple co-
154 morbidities and are at high risk of acute kidney injury due to colistin toxicity, any reduction
155 in the dose of colistin needed to achieve therapeutic activity would be extremely valuable
156 (32). Expression of MCR enzymes in our wild-type *E. coli* K-12 strain resulted in colistin
157 resistance (MIC of 3 μ g/mL or higher), while the strain harboring the empty vector was
158 sensitive to colistin (MIC of 1 μ g/mL). In almost all tested cases, the absence of DsbA caused
159 re-sensitization of the strains, as defined by the EUCAST breakpoint (*E. coli* strains with an
160 MIC of 2 μ g/mL or below are classified as susceptible) (Figure 1C), indicating that DsbA is
161 important for MCR function. Taking into consideration the challenges when using colistin
162 therapeutically (30-32), we conclude that deletion of *dsbA* led to clinically meaningful
163 decreases in colistin MIC values for tested MCR enzymes (Figure 1C), thus the role of DsbA
164 in MCR function should be further investigated.
165

166 Wild-type MIC values could be restored for all tested cysteine-containing enzymes by
167 complementation of *dsbA* (Figure 1 - figure supplements 4 and 5). Moreover, since DsbA
168 acts on its substrates post-translationally, we performed a series of control experiments
169 designed to assess whether the recorded effects were specific to the interaction of the
170 resistance proteins with DsbA, and not a result of a general inability of the *dsbA* mutant strain
171 to resist antibiotic stress. We observed no decreases in MIC values for the aminoglycoside
172 antibiotic gentamicin, which is not affected by the activity of the tested enzymes (Figure 1B,
173 Figure 1 - figure supplement 6). Furthermore, the β -lactam MIC values of strains harboring
174 the empty-vector alone, or a plasmid encoding L2-1 (Figure 1B), a β -lactamase containing
175 three cysteine residues, but no disulfide bond (PDB ID: 1O7E), remained unchanged. Finally,
176 to rule out the possibility that deletion of *dsbA* caused changes in cell envelope integrity that
177 might confound our results, we measured the permeability of the outer and inner membrane
178 of the *dsbA* mutant. To assess the permeability of the outer membrane, we used the
179 fluorescent dye 1-N-phenylnaphthylamine (NPN) and complemented our results with
180 vancomycin MIC assays (Figure 1 - figure supplement 7A). To test the integrity of the entire
181 cell envelope, we used the fluorescent dye propidium iodide (PI), as well as the β -
182 galactosidase substrate chlorophenyl red- β -D-galactopyranoside (CPRG) (Figure 1 - figure
183 supplement 7B). All four assays confirmed that the cell envelope integrity of the *dsbA* mutant
184 is comparable to the parental strain (Figure 1 - figure supplement 7). Together, these results
185 indicate that many cell envelope AMR determinants that contain more than one cysteine
186 residue are substrates of DsbA and that the process of disulfide bond formation is important
187 for their activity.

188
189 Unlike β -lactamases and MCR enzymes, none of the components of the six *E. coli* RND
190 efflux pumps contain periplasmic cysteine residues (33), and thus they are not substrates of
191 the DSB system. Nonetheless, as DsbA assists the folding of approximately 300
192 extracytoplasmic proteins, and plays a central role in maintaining the homeostasis of the cell
193 envelope proteome (21, 23, 24), we wanted to assess whether changes in periplasmic
194 proteostasis that occur in its absence could indirectly influence efflux pump function. To do
195 this we determined the MIC values of three antibiotics that are RND efflux pump substrates
196 using *E. coli* MG1655, a model strain for efflux studies, its *dsbA* mutant, and a mutant
197 lacking *acrA*, an essential component of the major *E. coli* RND pump AcrAB-TolC. MIC
198 values for the *dsbA* mutant were lower than for the parental strain for all tested substrate
199 antibiotics, but remained unchanged for the non-substrate gentamicin (Figure 1D). This
200 indicates that the MG1655 *dsbA* strain is generally able to resist antibiotic stress as efficiently
201 as its parent, and that the recorded decreases in MIC values are specific to defects in efflux
202 pump function in the absence of DsbA. As expected for a gene deletion of a pump
203 component, the *acrA* mutant had substantially lower MIC values for effluxed antibiotics
204 (Figure 1D). At the same time, even though gentamicin is not effluxed by AcrAB-TolC (34),
205 the gentamicin MIC of the *acrA* mutant is two-fold lower than that of *E. coli* MG1655, in
206 agreement with the fact that one of minor RND pump in *E. coli*, the aminoglycoside pump
207 AcrD, is entirely reliant on AcrA for its function (35-37). As before, the observed phenotype
208 could be reversed by complementation of *dsbA* (Figure 1 - figure supplement 8) and the
209 recorded effects were not due to changes in membrane permeability (Figure 1 - figure
210 supplement 9). Chloramphenicol is the only antibiotic from the tested efflux pump substrates
211 that has a EUCAST breakpoint for Gram-negative bacteria (*E. coli* strains with an MIC of 8
212 μ g/mL or below are classified as sensitive). It is notable that the MIC drop for this pump
213 substrate (Figure 1D), caused by deletion of *dsbA*, sensitized the *E. coli* MG1655 *dsbA* strain
214 to chloramphenicol (Figure 1E). Since mutations in *marR* that derepress MarA and cause
215 constitutive expression of AcrAB (38, 39) are observed in clinical isolates with increased

216 efflux (40), we constructed an *E. coli* MG1655 *marR* mutant to test the robustness of the
217 observed decrease in the chloramphenicol MIC in the absence of DsbA. We found that the
218 chloramphenicol MIC for the *dsbA marR* mutant remained below the EUCAST breakpoint
219 (Figure 1E), even when efflux pump components were overexpressed (Figure 1 - figure
220 supplement 10).

221 Overall, the effect of DsbA absence on efflux pump efficiency is less substantial than that
222 measured for a mutant lacking *acrA* (2-3-fold decrease in MIC versus 5-16-fold decrease,
223 respectively) (Figure 1D). Nonetheless, the recorded decreases in MIC values are robust
224 (Figure 1DE) and in agreement with previous studies reporting that deletion of *dsbA*
225 increases the sensitivity of *E. coli* to dyes like acridine orange and pyronin Y (18), which are
226 known substrates of AcrAB-TolC. While it is unlikely that the decreases in MIC values for
227 effluxed antibiotics in the absence of DsbA are of clinical significance, it is interesting to
228 explore the mechanistic relationship between DsbA and efflux pumps further, because there
229 are very few examples of DsbA being important for the function of extra-cytoplasmic
230 proteins independently of its disulfide bond forming capacity (41, 42).

231
232
233 *Altered periplasmic proteostasis due to the absence of DsbA results in degradation or*
234 *misfolding of cysteine-containing resistance determinants and sub-optimal function of efflux*
235 *pumps*

236 To understand the underlying mechanisms that result in the decreased MIC values observed
237 for the *dsbA* mutant strains, we assessed the protein levels of a representative subset of β -
238 lactamases (GES-1, L1-1, KPC-3, FRI-1, OXA-4, OXA-10, OXA-198) and all tested MCR
239 enzymes by immunoblotting. When expressed in the *dsbA* mutant, all Ambler class A and B
240 β -lactamases (Table 1), except GES-1 which we were not able to visualize by
241 immunoblotting, exhibited drastically reduced protein levels whilst the amount of the control
242 enzyme L2-1 remained unaffected (Figure 2A). This suggests that when these enzymes lack
243 their disulfide bond, they are unstable and ultimately degraded. We did not detect any
244 decrease in protein amounts for Ambler class D enzymes (Table 1, Figure 2B). However, the
245 hydrolytic activity of these β -lactamases was significantly lower in the *dsbA* mutant (Figure
246 2C), suggesting a folding defect that leads to loss of function.

247
248 Like with class A and B β -lactamases, MCR enzymes were undetectable when expressed in a
249 *dsbA* mutant (Figure 3A) suggesting that their stability is severely compromised when they
250 lack their disulfide bonds. We further confirmed this by directly monitoring the lipid A
251 profile of all MCR-expressing strains where deletion of *dsbA* resulted in colistin MIC values
252 of 2 μ g/mL or lower (i.e., strains expressing MCR-3, -4, -5 and -8, Figure 1C) using MALDI-
253 TOF mass spectrometry (Figure 3BC). MCR activity leads to the addition of
254 phosphoethanolamine to the lipid A portion of bacterial lipopolysaccharide (LPS), resulting
255 in reduced binding of colistin to LPS and, thus, resistance. In *E. coli* the major lipid A peak
256 detected by mass spectrometry is present at *m/z* 1796.2 (Figure 3B, first spectrum) and it
257 corresponds to hexa-acyl diphosphoryl lipid A (native lipid A). The lipid A profile of *E. coli*
258 MC1000 *dsbA* was identical to that of the parental strain (Figure 3B, second spectrum). In the
259 presence of MCR enzymes two additional peaks were observed, at *m/z* 1821.2 and 1919.2
260 (Figure 3B, third spectrum). The peak at *m/z* 1919.2 corresponds to the addition of a
261 phosphoethanolamine moiety to the phosphate group at position 1 of native lipid A, and the
262 peak at *m/z* 1821.2 corresponds to the addition of a phosphoethanolamine moiety to the 4'
263 phosphate of native lipid A and the concomitant loss of the phosphate group at position 1
264 (43). For *dsbA* mutants expressing MCR-3, -5 and -8 (Figure 3C), the peaks at *m/z* 1821.2

266 and m/z 1919.2 could no longer be detected, whilst the native lipid A peak at m/z 1796.2
267 remained unchanged (Figure 3B, fourth spectrum); *dsbA* mutants expressing MCR-4 retain
268 some basal lipid A-modifying activity, nonetheless this is not sufficient for this strain to
269 efficiently evade colistin treatment (Figure 1C). Together these data suggest that in the
270 absence of DsbA, MCR enzymes are unstable (Figure 3A) and therefore no longer able to
271 efficiently catalyze the addition of phosphoethanolamine to native lipid A (Figure 3BC); as a
272 result, they cannot confer resistance to colistin (Figure 1C).

273

274 As RND efflux pump proteins do not contain any disulfide bonds, the decreases in MIC
275 values for pump substrates in the absence of *dsbA* (Figure 1D) are likely mediated by
276 additional cell-envelope components. The protease DegP, previously found to be a DsbA
277 substrate (20), seemed a promising candidate for linking DsbA to efflux pump function.
278 DegP degrades a range of misfolded extracytoplasmic proteins including, but not limited to,
279 subunits of higher order protein complexes and proteins lacking their native disulfide bonds
280 (44). We hypothesized that in a *dsbA* mutant the substrate burden on DegP would be
281 dramatically increased, whilst DegP itself would not function optimally due to absence of its
282 disulfide bond (45). Consequently, protein turn over in the cell envelope would not occur
283 efficiently. Since the essential RND efflux pump component AcrA needs to be cleared by
284 DegP when it becomes misfolded or nonfunctional (46), we expected that the reduced DegP
285 efficiency in a *dsbA* mutant would result in accumulation of nonfunctional AcrA in the
286 periplasm, which would then interfere with pump function. In agreement with our hypothesis,
287 we found that in the absence of DsbA degradation of DegP occurred, reducing the pool of
288 active enzyme (Figure 4A) (45). In addition, AcrA accumulated to the same extent in a *dsbA*
289 and a *degP* mutant (Figure 4B), suggesting that in both these strains AcrA was not efficiently
290 cleared. Finally, no accumulation was detected for the outer-membrane protein TolC, which
291 is not a DegP substrate (Figure 4C) (47). Thus, in the absence of DsbA, inefficient DegP-
292 mediated periplasmic proteostasis impacts RND efflux pump function (Figure 1D) through
293 the accumulation of AcrA that should have been degraded and removed from the cell
294 envelope.

295

296 The data presented above validate our initial hypothesis. The absence of DsbA affects the
297 stability and folding of cysteine-containing resistance proteins and in most cases leads to
298 drastically reduced protein levels for the tested enzymes. As a result, and in agreement with
299 the recorded decreases in MIC values (Figure 1BC), these folding defects impede the ability
300 of AMR determinants to confer resistance (Figure 4B). At the same time, changes in cell
301 envelope protein homeostasis have a clear effect on protein function in this compartment, as
302 demonstrated by the fact that prevention of disulfide bond formation indirectly impairs the
303 efficiency of the AcrAB-TolC efflux pump (Figure 1DE and 4D).

304

305 *Sensitization of clinical isolates to existing antibiotics can be achieved by chemical inhibition*
306 *of DsbA activity*

307

308 DsbA is essential for the folding of many virulence factors. As such, inhibition of the DSB
309 system has been proposed as a promising anti-virulence strategy (25-27) and efforts have
310 been made to develop inhibitors for DsbA (48, 49), its redox partner DsbB (Figure 1A) (50)
311 or both (51). These studies have made the first steps towards the production of chemical
312 compounds that inhibit the function of the DSB proteins, providing us with a laboratory tool
313 to test our approach against AMR.

314

315 4,5-dichloro-2-(2-chlorobenzyl)pyridazin-3-one, termed “compound 12” in Landeta et al.
316 (50) is a potent laboratory inhibitor of *E. coli* DsbB and its analogues from closely related
317 organisms. Using this molecule, we could chemically inhibit the function of the DSB system.
318 We first tested the motility of *E. coli* MC1000 in the presence of the inhibitor and found that
319 cells were significantly less motile (Figure 5AB), consistent with the fact that impairing DSB
320 function prevents the formation of the flagellar P-ring component FlgI (52, 53). Furthermore,
321 we directly assessed the redox state of DsbA in the presence of “compound 12” to probe
322 whether it was being re-oxidized by DsbB, a necessary step that occurs after each round of
323 oxidative protein folding and allows DsbA to remain active (Figure 1A). Under normal
324 growth conditions, DsbA was in its active oxidized form in the bacterial periplasm (i.e., C30
325 and C33 form a disulfide bond), showing that it was efficiently regenerated by DsbB (54)
326 (Figure 5C). By contrast, addition of the inhibitor to growing *E. coli* MC1000 cells resulted
327 in accumulation of inactive reduced DsbA, thus confirming that DsbB function was impeded
328 (Figure 5C).

329
330 After testing the efficacy of the DsbB inhibitor, we proceeded to examine whether chemical
331 inhibition of the DSB system could be used to broadly impair the function of AMR
332 determinants. We determined MIC values for the latest generation β -lactam that each β -
333 lactamase can hydrolyze, or colistin, for our panel of *E. coli* MC1000 strains and found that
334 addition of the compound during MIC testing phenocopied the effects of a *dsbA* deletion on
335 β -lactamase and MCR activity (Figure 5DE, Figure 5 - figure supplement 1). The observed
336 effects are not a result of altered cell growth, as addition of the compound does not affect the
337 growth profile of the bacteria (Figure 5 - figure supplement 2A), in agreement with the fact
338 that deletion of *dsbA* does not affect cell viability (Figure 5 - figure supplement 2B).
339 Furthermore, the changes in the recorded MIC values are due solely to inhibition of the DSB
340 system as no additive effects on MIC values were observed when the *dsbA* mutant harboring
341 a β -lactamase or *mcr* gene was exposed to the compound (Figure 5 - figure supplement 3).

342
343 Having shown that the DSB system is a tractable target in the context of AMR, we examined
344 the effect of chemical inhibition on several species of β -lactamase-expressing Enterobacteria
345 (Supplementary Table 3). DSB system inhibition in a clinical isolate of *Klebsiella*
346 *pneumoniae* expressing KPC-2 sensitized the strain to imipenem as defined by EUCAST
347 breakpoints (Figure 6A). The efficiency of this double treatment is evident from scanning
348 electron micrographs of the tested strains (Figure 6B). Addition of either the DSB system
349 inhibitor or imipenem alone does not cause any changes in the morphology of *K. pneumoniae*
350 cells, which remain healthy and dividing (Figure 6B, top row). By contrast, the combination
351 of the inhibitor with imipenem (added at a sub-MIC final concentration of 6 μ g/mL), led to
352 dramatic changes in the appearance of the cells, whose integrity was entirely compromised
353 (Figure 6B, bottom row). Furthermore, *E. coli* and *Citrobacter freundii* isolates expressing
354 KPC-2, including multidrug-resistant strains, also showed clinically relevant decreases in
355 their MIC values for imipenem that resulted in sensitization when their DSB system was
356 chemically inhibited (Figure 6C). For an *Enterobacter cloacae* isolate expressing FRI-1,
357 chemical inhibition of DsbA caused a reduction in the aztreonam MIC value by over 180
358 μ g/mL, resulting in intermediate resistance as defined by EUCAST breakpoints (Figure 6D).
359 Along with β -lactamase-expressing strains, we also tested the effect of DsbA inhibition on
360 MCR-producing clinical isolates. We found that combination of the DSB system inhibitor
361 with colistin led to reduction of the colistin MIC and sensitization of MCR-1-expressing *E.*
362 *coli* (Figure 6E). In agreement with this, SEM images of this strain after combination
363 treatment using sub-MIC amounts of colistin (final concentration of 2 μ g/mL) revealed
364 drastic changes in morphology, whereby cells blebbed intensely or their contents leaked out

365 (Figure 6F). We tested four more clinical *E. coli* isolates producing diverse MCR enzymes
366 and found that also for these strains DSB system inhibition allowed sensitization to colistin
367 (Figure 6G, Figure 6 - figure supplement 1). At the same time, we were able to show that
368 DSB system inhibition in *E. coli* CNR1790 (i.e., the clinical isolate expressing both MCR-1
369 and the ESBL TEM-15 that was sensitized to colistin in Figure 6E), led to a decrease in its
370 ceftazidime MIC, resulting in intermediate resistance (Figure 6H). While we did not test the
371 dependence of TEM enzymes on DsbA in our panel of *E. coli* K-12 strains, we chose to test
372 the effects of DSB system inhibition on *E. coli* CNR1790 because we posited that the
373 disulfide bond in TEM-15 may be important for its function, based on the fact that TEM-1
374 has been shown to be reliant on its disulfide under stress conditions (29). Validation of our
375 hypothesis provides evidence that DsbA inhibition can improve the resistance profile of the
376 same isolate both for β -lactam (Figure 6H) and polymyxin (Figure 6E) antibiotics. Together,
377 these results, obtained using multiple clinical strains from several bacterial species, provide
378 further validation of the significance of our data from heterologously expressed β -lactamase
379 and MCR enzymes in *E. coli* K-12 strains (Figure 1BC), and showcase the potential of this
380 approach for clinical applications.

381
382 To determine if our approach for Enterobacteria would be appropriate for other multidrug-
383 resistant pathogens we tested it on *Pseudomonas aeruginosa*. This bacterium has two DsbB
384 analogues which are functionally redundant (55). The chemical inhibitor used in this study
385 has been shown to be effective against DsbB1, but less effective against DsbB2 of *P.*
386 *aeruginosa* PA14 (50), making it unsuitable for MIC assays on *P. aeruginosa* clinical isolates.
387 Nonetheless, deletion of *dsbA1* in a multidrug-resistant *P. aeruginosa* clinical isolate
388 expressing OXA-198 (PA43417), led to sensitization of this strain to the antipseudomonal β -
389 lactam piperacillin (Figure 7A). In addition, we deleted *dsbA1* in the multidrug-resistant *P.*
390 *aeruginosa* PAe191 strain that produces OXA-19, a member of the OXA-10 phylogenetic
391 family (Supplementary Table 1) and the most disseminated OXA enzyme in clinical strains
392 (56). In this case, absence of DsbA caused a drastic reduction in the ceftazidime MIC value
393 by over 220 μ g/mL, and sensitized the strain to aztreonam (Figure 7B). These results suggest
394 that targeting disulfide bond formation could be useful for the sensitization of many more
395 clinically important Gram-negative species.

396
397 Finally, to test our approach in an infection context we performed *in vivo* survival assays
398 using the wax moth model *Galleria mellonella* (Figure 7C). Larvae were infected with the *P.*
399 *aeruginosa* PAe191 clinical isolate producing OXA-19, and its *dsbA1* mutant, and infections
400 were treated once with ceftazidime at a final concentration below the EUCAST breakpoint,
401 as appropriate. No larvae survived 18 hours post infection with *P. aeruginosa* PAe191, even
402 when treatment with ceftazidime was performed (Figure 7C, blue and red survival curves).
403 Deletion of *dsbA1* resulted in 80% mortality of the larvae at 50 hours post infection (Figure
404 7C, light blue survival curve); this increase in survival compared to larvae infected with *P.*
405 *aeruginosa* PAe191 is due to the fact that absence of the principal DsbA protein likely affects
406 the virulence of the pathogen (57). Nonetheless, treatment of the *dsbA1* mutant with
407 ceftazidime resulted in a significant increase in survival (17% mortality) compared to the
408 untreated condition 50 hours post infection (Figure 7C, compare the light blue and pink
409 survival curves). This improvement in survival is even more noticeable if one compares the
410 survival of larvae treated with ceftazidime after infection with *P. aeruginosa* PAe191 versus
411 infection with *P. aeruginosa* PAe191 *dsbA1* (Figure 7C, compare the red and pink survival
412 curves). Since OXA-19, in this case produced by a multi-drug resistant clinical strain
413 (Supplementary Table 3, Figure 7B), is a broad-spectrum β -lactamase that cannot be

414 neutralized by classical β -lactamase inhibitors (Table 1), these results further highlight the
415 promise of our approach for future clinical applications.

416 **DISCUSSION**

417
418 This work is one of the first reports of a strategy capable of simultaneously impairing
419 multiple types of AMR determinants by compromising the function of a single target. By
420 inhibiting DsbA, a non-essential cell envelope protein which is unique to bacteria, we can
421 inactivate diverse resistance enzymes and sensitize critically important pathogens to multiple
422 classes of existing antibiotics. This proof of principle will hopefully further incentivize the
423 development of DsbA inhibitors and open new avenues towards the inception of novel
424 adjuvants that will help reverse AMR in Gram-negative organisms.

425
426 We have shown that targeting DsbA incapacitates broad-spectrum β -lactamases from three of
427 the four Ambler classes (class A, B and D, Figure 1B). This includes enzymes that are not
428 susceptible to classical β -lactamase inhibitors (Table 1), such as members of the KPC and
429 OXA families, as well as metallo- β -lactamases like L1-1 from the often pan-resistant
430 organism *Stenotrophomonas maltophilia*. The function of these proteins is impaired without a
431 small molecule binding to their active site, unlike the currently-used β -lactamase inhibitors
432 which often generate resistance (4). As DsbA dependence is conserved within phylogenetic
433 groups (Figure 1 - figure supplement 2), based on the number of enzymes belonging to the
434 same phylogenetic family as the β -lactamases tested in this study (Supplementary Table 1),
435 we anticipate that a total of 195 discrete enzymes rely on DsbA for their stability and
436 function, 84 of which cannot be inhibited by classical adjuvant approaches. DsbA is widely
437 conserved (25), thus targeting the DSB system should not only compromise β -lactamases in
438 Enterobacteria but, as demonstrated by our experiments using *P. aeruginosa* clinical isolates
439 (Figure 7), could also be a promising avenue for impairing the function of AMR determinants
440 expressed by other highly-resistant Gram-negative organisms. As such, together with the fact
441 that approximately 56% of the β -lactamase phylogenetic families found in pathogens and
442 organisms capable of causing opportunistic infections contain enzymes with two or more
443 cysteines (Supplementary Table 1), we expect many more clinically relevant β -lactamases,
444 beyond those already tested in this study, to depend on DsbA.

445
446 MCR enzymes are rapidly becoming a grave threat to the use of colistin (13), a drug of last
447 resort often needed for the treatment of multidrug-resistant infections (11). Currently,
448 experimental inhibitors of these proteins are sparse and poorly characterized (58), and only
449 one existing compound, the antirheumatic drug auranofin, seems to successfully impair MCR
450 enzymes (through displacement of their zinc cofactor) (59). As all MCR members contain
451 multiple disulfide bonds, inhibition of the DSB system provides a broadly applicable solution
452 for reversing MCR-mediated colistin resistance (Figure 1C, 5E and 6EFG) that would likely
453 extend to novel MCR proteins that may emerge in the future. Since the decrease in colistin
454 MIC values upon *dsbA* deletion (Figure 1C) or DsbB inhibition (Figure 5E and 6EFG) is
455 modest, this phenotype cannot be used in future screens aiming to identify DsbA inhibitors,
456 because such applications require a larger than 4-fold decrease in recorded MIC values to
457 reliably identify promising hits. Nonetheless, our findings in this study clearly demonstrate
458 that absence of DsbA results in degradation of MCR enzymes and abrogation of their
459 function (Figure 3), which, in turn, leads to sensitization of all tested *E. coli* clinical isolates
460 to colistin (Figure 6EFG). This adds to other efforts aiming to reduce the colistin MIC of
461 polymyxin resistant strains (60, 61). As such, if a clinically useful DsbA inhibitor were to
462 become available, it would be valuable to test its efficacy against large panels of MCR-
463 expressing clinical strains, as it might offer a new way to bypass MCR-mediated colistin
464 resistance.

465

466 No clinically applicable efflux pump inhibitors have been identified to date (62) despite many
467 efforts to use these macromolecular assemblies as targets against intrinsic resistance. While
468 deletion of *dsbA* sensitizes the tested *E. coli* strain to chloramphenicol (Figure 1E), the
469 overall effects of DsbA absence on efflux function are modest (Figure 1D). That said, our
470 results regarding the relationship between DsbA-mediated proteostasis and pump function
471 (Figure 4A-C) highlight the importance of other cell envelope proteins responsible for protein
472 homeostasis, like DegP, for bacterial efflux. Since the cell envelope contains multiple protein
473 folding catalysts (16), it would be worth investigating if other redox proteins, chaperones or
474 proteases could be targeted to indirectly compromise efflux pumps.
475

476 More generally, our findings demonstrate that cell envelope proteostasis pathways have
477 significant, yet untapped, potential for the development of novel antibacterial strategies. The
478 example of the DSB system presented here is particularly telling. This pathway, initially
479 considered merely a housekeeping system (63), plays a major role in clinically relevant
480 bacterial niche adaptation. In addition to assisting the folding of 40% of the cell-envelope
481 proteome (23, 24), the DSB system is essential for virulence (25, 26), has a key role in the
482 formation and awakening of bacterial persister cells (64) and, as seen in this work, is required
483 for bacterial survival in the presence of widely used antibiotic compounds. As shown in our
484 *in vivo* experiments (Figure 7C), targeting such a system in Gram-negative pathogens could
485 lead to adjuvant approaches that inactivate AMR determinants whilst simultaneously
486 incapacitating an arsenal of virulence factors. Therefore, this study not only lays the
487 groundwork for future clinical applications, such as the development of broad-acting
488 antibiotic adjuvants, but also serves as a paradigm for exploiting other accessible cell
489 envelope proteostasis processes for the design of next-generation therapeutics.

490 **MATERIALS AND METHODS**

491

492 **Reagents and bacterial growth conditions.** Unless otherwise stated, chemicals and reagents
493 were acquired from Sigma Aldrich, growth media were purchased from Oxoid and antibiotics
494 were obtained from Melford Laboratories. Lysogeny broth (LB) (10 g/L NaCl) and agar
495 (1.5% w/v) were used for routine growth of all organisms at 37 °C with shaking at 220 RPM,
496 as appropriate. Unless otherwise stated, Mueller-Hinton (MH) broth and agar (1.5% w/v)
497 were used for Minimum Inhibitory Concentration (MIC) assays. Growth media were
498 supplemented with the following, as required: 0.25 mM Isopropyl β -D-1-
499 thiogalactopyranoside (IPTG) (for strains harboring β -lactamase-encoding pDM1 plasmids),
500 0.5 mM IPTG (for strains harboring MCR-encoding pDM1 plasmids), 12.5 μ g/mL
501 tetracycline, 100 μ g/mL ampicillin, 50 μ g/mL kanamycin, 10 μ g/mL gentamicin, 33 μ g/mL
502 chloramphenicol, 50 μ g/mL streptomycin (for cloning purposes), and 2000-5000 μ g/mL
503 streptomycin (for the construction of *Pseudomonas aeruginosa* mutants).

504

505 **Construction of plasmids and bacterial strains.** Bacterial strains and plasmids used in this
506 study are listed in the Key Resources Table and in Supplementary Tables 4 and 5,
507 respectively. Oligonucleotides used in this study are listed in Supplementary Table 6. DNA
508 manipulations were conducted using standard methods. KOD Hot Start DNA polymerase
509 (Merck) was used for all PCR reactions according to the manufacturer's instructions,
510 oligonucleotides were synthesized by Sigma Aldrich and restriction enzymes were purchased
511 from New England Biolabs. All DNA constructs were sequenced and confirmed to be correct
512 before use.

513

514 Genes for β -lactamase and MCR enzymes were amplified from genomic DNA extracted from
515 clinical isolates (Supplementary Table 7) with the exception of *mcr-3* and *mcr-8*, which were
516 synthesized by GeneArt Gene Synthesis (ThermoFisher Scientific). β -lactamase and MCR
517 genes were cloned into the IPTG-inducible plasmid pDM1 using primers P1-P36. pDM1
518 (GenBank accession number MN128719) was constructed from the p15A-*ori* plasmid
519 pACYC184 (65) to contain the Lac repressor, the *Ptac* promoter, an optimized ribosome
520 binding site and a multiple cloning site (NdeI, SacI, PstI, KpnI, XhoI and XmaI) inserted into
521 the NcoI restriction site of pACYC184. All StrepII-tag fusions of β -lactamase and MCR
522 enzymes (constructed using primers P1, P3, P9, P11, P13, P15, P17, P21, P23, P25, P27,
523 P29, P37, P38 and P41-P50) have a C-terminal StrepII tag (GSAWSHPQFEK) except for
524 OXA-4, where an N-terminal StrepII tag was inserted between the periplasmic signal
525 sequence and the body of the protein using the primer pairs P7/P40, P9/P39 and P7/P8.
526 Plasmids encoding *ges-1*, *kpc-3* and *mcr-3.2* were obtained by performing QuickChange
527 mutagenesis on pDM1 constructs encoding *ges-5*, *kpc-2* and *mcr-3*, respectively (primers
528 P31-P36).

529

530 *E. coli* gene mutants were constructed using a modified lambda-Red recombination method,
531 as previously described (66) (primers P53-P62). To complement the *dsbA* mutant, a DNA
532 fragment consisting of *dsbA* preceded by the *Ptac* promoter was inserted into the NotI/XhoI
533 sites of pGRG25 (primers P51/P52) and was reintroduced into the *E. coli* chromosome at the
534 *attTn7* site, as previously described (67). The *dsbA1* mutants of the *P. aeruginosa* PA43417
535 and *P. aeruginosa* PAe191 clinical isolates were constructed by allelic exchange, as
536 previously described (68). Briefly, the *dsbA1* gene area of *P. aeruginosa* PA43417 and *P.*
537 *aeruginosa* PAe191 (including the *dsbA1* gene and 600 bp on either side of this gene) was
538 amplified (primers P63/P64) and the obtained DNA was sequenced to allow for accurate
539 primer design for the ensuing cloning step. Subsequently, 500-bp DNA fragments upstream

540 and downstream of the *dsbA1* gene were amplified using *P. aeruginosa* PA43417 genomic
541 DNA (primers P65/P66 (upstream) and P67/P68 (downstream)). A fragment containing both
542 regions was obtained by overlapping PCR (primers P65/P68) and inserted into the
543 *Xba*I/*Bam*HI sites of pKNG101. The suicide vector pKNG101 (69) is not replicative in *P.*
544 *aeruginosa*; it was maintained in *E. coli* CC118λpir and mobilized into *P. aeruginosa*
545 PA43417 and *P. aeruginosa* PAe191 by triparental conjugation.

546

547 ***MIC assays.*** Unless otherwise stated, antibiotic MIC assays were carried out in accordance
548 with the EUCAST recommendations using ETEST strips (BioMérieux). Briefly, overnight
549 cultures of each strain to be tested were standardized to OD₆₀₀ 0.063 in 0.85% NaCl
550 (equivalent to McFarland standard 0.5) and distributed evenly across the surface of MH agar
551 plates. ETEST strips were placed on the surface of the plates, evenly spaced, and the plates
552 were incubated for 18-24 hours at 37 °C. MICs were read according to the manufacturer's
553 instructions. β-lactam MICs were also determined using the Broth Microdilution (BMD)
554 method, as required. Briefly, a series of antibiotic concentrations was prepared by two-fold
555 serial dilution in MH broth in a clear-bottomed 96-well microtiter plate (Corning). When
556 used, tazobactam was included at a fixed concentration of 4 µg/mL in every well, in
557 accordance with the EUCAST guidelines. The strain to be tested was added to the wells at
558 approximately 5 x 10⁴ colony forming units (CFU) per well and plates were incubated for 18-
559 24 hours at 37 °C. The MIC was defined as the lowest antibiotic concentration with no
560 visible bacterial growth in the wells. Vancomycin MICs were determined using the BMD
561 method, as above. All colistin sulphate MIC assays were performed using the BMD method
562 as described above except that instead of two-fold serial dilutions, the following
563 concentrations of colistin (Acros Organics) were prepared individually in MH broth: 8
564 µg/mL, 7 µg/mL, 6 µg/mL, 5.5 µg/mL, 5 µg/mL, 4.5 µg/mL, 4 µg/mL, 3.5 µg/mL, 3 µg/mL,
565 2.5 µg/mL, 2 µg/mL, 1.5 µg/mL, 1 µg/mL, 0.5 µg/mL.

566

567 The covalent DsbB inhibitor 4,5-dichloro-2-(2-chlorobenzyl)pyridazin-3-one (50) was used
568 to chemically impair the function of the DSB system. Inactivation of DsbB results in
569 abrogation of DsbA function (54) only in media free of small-molecule oxidants (52).
570 Therefore, MIC assays involving chemical inhibition of the DSB system were performed
571 using M63 broth (15.1 mM (NH₄)₂SO₄, 100 mM KH₂PO₄, 1.8 mM FeSO₄.7H₂O, adjusted to
572 pH 7.2 with KOH) and agar (1.5% w/v) supplemented with 1 mM MgSO₄, 0.02% w/v
573 glucose, 0.005% w/v thiamine, 31 µM FeCl₃.6H₂O, 6.2 µM ZnCl₂, 0.76 µM CuCl₂.2H₂O,
574 1.62 µM H₃BO₃, 0.081 µM MnCl₂.4H₂O, 84.5 mg/L alanine, 19.5 mg/L arginine, 91 mg/L
575 aspartic acid, 65 mg/L glutamic acid, 78 mg/L glycine, 6.5 mg/L histidine, 26 mg/L
576 isoleucine, 52 mg/L leucine, 56.34 mg/L lysine, 19.5 mg/L methionine, 26 mg/L
577 phenylalanine, 26 mg/L proline, 26 mg/L serine, 6.5 mg/L threonine, 19.5 mg/L tyrosine,
578 56.34 mg/L valine, 26 mg/L tryptophan, 26 mg/L asparagine and 26 mg/L glutamine. CaCl₂
579 was also added at a final concentration of 0.223 mM for colistin sulfate MIC assays. Either
580 DMSO (vehicle control) or the covalent DsbB inhibitor 4,5-dichloro-2-(2-
581 chlorobenzyl)pyridazin-3-one (final concentration of 50 µM) (Enamine) (50) were added to
582 the M63 medium, as required. The strain to be tested was added at an inoculum that
583 recapitulated the MH medium MIC values obtained for that strain.

584

585 ***SDS-PAGE analysis and immunoblotting.*** Samples for immunoblotting were prepared as
586 follows. Strains to be tested were grown on LB or MH agar plates as lawns in the same
587 manner as for MIC assays described above. Bacteria were collected using an inoculating loop
588 and resuspended in 0.85% NaCl or LB to OD₆₀₀ 2.0 (except for strains expressing OXA-4,
589 where OD₆₀₀ 6.0 was used). For strains expressing β-lactamase enzymes, the cell suspensions

590 were spun at 10,000 $\times g$ for 10 minutes and bacterial pellets were lysed by addition of
591 BugBuster Master Mix (Merck Millipore) for 25 minutes at room temperature with gentle
592 agitation. Subsequently, lysates were spun at 10,000 $\times g$ for 10 minutes at 4 °C and the
593 supernatant was added to 4 x Laemmli buffer. For strains expressing MCR enzymes cell
594 suspensions were directly added to 4 x Laemmli buffer, while for *E. coli* MG1655 and its
595 mutants, cells were lysed as above and lysates were added to 4 x Laemmli buffer. All
596 samples were boiled for 5 minutes before separation by SDS-PAGE.
597

598 Unless otherwise stated, SDS-PAGE analysis was carried out using 10% BisTris NuPAGE
599 gels (ThermoFisher Scientific) using MES/SDS running buffer prepared according to the
600 manufacturer's instructions and including pre-stained protein markers (SeeBlue Plus 2,
601 ThermoFisher Scientific). Proteins were transferred to Amersham Protran nitrocellulose
602 membranes (0.45 μ m pore size, GE Life Sciences) using a Trans-Blot Turbo transfer system
603 (Bio-Rad) before blocking in 3% w/v Bovine Serum Albumin (BSA)/TBS-T (0.1 % v/v
604 Tween 20) or 5% w/v skimmed milk/TBS-T and addition of primary and secondary
605 antibodies. The following primary antibodies were used in this study: Strep-Tactin-HRP
606 conjugate (Iba Lifesciences) (dilution 1:3,000 in 3 w/v % BSA/TBS-T), Strep-Tactin-AP
607 conjugate (Iba Lifesciences) (dilution 1:3,000 in 3 w/v % BSA/TBS-T), rabbit anti-DsbA
608 antibody (dilution 1:1,000 in 5 w/v % skimmed milk/TBS-T), rabbit anti-AcrA antibody
609 (dilution 1:10,000 in 5 w/v % skimmed milk/TBS-T), rabbit anti-TolC antibody (dilution
610 1:5,000 in 5 w/v % skimmed milk/TBS-T), rabbit anti-HtrA1 (DegP) antibody (Abcam)
611 (dilution 1:1,000 in 5 w/v % skimmed milk/TBS-T) and mouse anti-DnaK 8E2/2 antibody
612 (Enzo Life Sciences) (dilution 1:10,000 in 5% w/v skimmed milk/TBS-T). The following
613 secondary antibodies were used in this study: goat anti-rabbit IgG-AP conjugate (Sigma
614 Aldrich) (dilution 1:6,000 in 5% w/v skimmed milk/TBS-T), goat anti-rabbit IgG-HRP
615 conjugate (Sigma Aldrich) (dilution 1:6,000 in 5% w/v skimmed milk/TBS-T), goat anti-
616 mouse IgG-AP conjugate (Sigma Aldrich) (dilution 1:6,000 in 5% w/v skimmed milk/TBS-
617 T) and goat anti-mouse IgG-HRP conjugate (Sigma Aldrich) (dilution 1:6,000 in 5% w/v
618 skimmed milk/TBS-T). Membranes were washed three times for 5 minutes with TBS-T prior
619 to development. Development for AP conjugates was carried out using a SigmaFast
620 BCIP/NBT tablet, while HRP conjugates were visualized with the Novex ECL HRP
621 chemiluminescent substrate reagent kit (ThermoFisher Scientific) or the Immobilon
622 Crescendo chemiluminescent reagent (Merck) using a Gel Doc XR+ Imager (Bio-Rad).
623

624 **β -lactam hydrolysis assay.** β -lactam hydrolysis measurements were carried out using the
625 chromogenic β -lactam nitrocefin (Abcam). Briefly, overnight cultures of strains to be tested
626 were centrifugated, pellets were weighed and resuspended in 150 μ L of 100 mM sodium
627 phosphate buffer (pH 7.0) per 1 mg of wet-cell pellet, and cells were lysed by sonication. For
628 strains harboring pDM1, pDM1-*bla*_{L2-1}, pDM1-*bla*_{OXA-10} and pDM1-*bla*_{GES-1}, lysates
629 corresponding to 0.34 mg of bacterial pellet were transferred into clear-bottomed 96-well
630 microtiter plates (Corning). For strains harboring pDM1-*bla*_{OXA-4} and pDM1-*bla*_{OXA-198},
631 lysates corresponding to 0.2 mg and 0.014 mg of bacterial pellet were used, respectively. In
632 all cases, nitrocefin was added at a final concentration of 400 μ M and the final reaction
633 volume was made up to 100 μ L using 100 mM sodium phosphate buffer (pH 7.0). Nitrocefin
634 hydrolysis was monitored at 25 °C by recording absorbance at 490 nm at 60-second intervals
635 for 15 minutes using an Infinite M200 Pro microplate reader (Tecan). The amount of
636 nitrocefin hydrolyzed by each lysate in 15 minutes was calculated using a standard curve
637 generated by acid hydrolysis of nitrocefin standards.
638

639 **NPN uptake assay.** 1-N-phenylnaphthylamine (NPN) (Acros Organics) uptake assays were
640 performed as described by Helander & Mattila-Sandholm (70). Briefly, mid-log phase
641 cultures of strains to be tested were diluted to OD₆₀₀ 0.5 in 5 mM HEPES (pH 7.2) before
642 transfer to clear-bottomed 96-well microtiter plates (Corning) and addition of NPN at a final
643 concentration of 10 μ M. Colistin sulphate (Acros Organics) was included at a final
644 concentration of 0.5 μ g/mL, as required. Immediately after the addition of NPN, fluorescence
645 was measured at 60-second intervals for 10 minutes using an Infinite M200 Pro microplate
646 reader (Tecan); the excitation wavelength was set to 355 nm and emission was recorded at
647 405 nm.

648

649 **PI uptake assay.** Exponentially-growing (OD₆₀₀ 0.4) *E. coli* strains harboring pUltraGFP-GM
650 (71) were diluted to OD₆₀₀ 0.1 in phosphate buffered saline (PBS) (pH 7.4) and cecropin A
651 was added to a final concentration of 20 μ M, as required. Cell suspensions were incubated at
652 room temperature for 30 minutes before centrifugation and resuspension of the pellets in
653 PBS. Propidium iodide (PI) was then added at a final concentration of 3 μ M. Suspensions
654 were incubated for 10 minutes at room temperature and analyzed on a two-laser, four color
655 BD FACSCalibur flow cytometer (BD Biosciences). 50,000 events were collected for each
656 sample and data were analyzed using FlowJo v.10.0.6 (Treestar).

657

658 **CPRG hydrolysis assay.** The cell envelope integrity of bacterial strains used in this study and
659 of their *dsbA* mutants, was tested by measuring the hydrolysis of the β -galactosidase substrate
660 chlorophenyl red- β -D-galactopyranoside (CPRG) by cytoplasmic LacZ, as previously
661 described (72). Briefly, exponentially growing (OD₆₀₀ 0.4) *E. coli* MC1000 harboring
662 pCB112 or MG1655, as well as their *dsbA* mutants, were diluted to 1:10⁵ in MH broth and
663 plated on MH agar containing CPRG and IPTG at final concentrations of 20 μ g/mL and 50
664 μ M, respectively. Plates were incubated at 37°C for 18 hours, were photographed, and
665 images were analyzed using Adobe Photoshop CS4 extended v.11.0 (Adobe) as follows.
666 Images were converted to CMYK color space format, colonies were manually selected using
667 consistent tolerance (26, anti-alias, contiguous) and edge refinement (32 px, 100% contrast),
668 and the magenta color was quantified for each image and normalized for the area occupied by
669 each colony.

670

671 **MALDI-TOF Mass spectrometry.** Lipid A profiles of strains to be tested were determined
672 using intact bacteria, as previously described (73). The peak for *E. coli* native lipid A is
673 detected at *m/z* 1796.2, whereas the lipid A profiles of strains expressing functional MCR
674 enzymes have two additional peaks, at *m/z* 1821.2 and 1919.2. These peaks result from
675 MCR-mediated modification of native lipid A through addition of phosphoethanolamine
676 moieties (43). The ratio of modified to unmodified lipid A was calculated by summing the
677 intensities of the peaks at *m/z* 1821.2 and 1919.2 and dividing this value by the intensity of
678 the native lipid A peak at *m/z* 1796.2.

679

680 **Motility assay.** 500 μ L of overnight culture of each strain to be tested were centrifuged and
681 the pellets were washed three times in M63 broth before resuspension in the same medium to
682 achieve a final volume of 25 μ L. Bacterial motility was assessed by growth in M63 medium
683 containing 0.25% w/v agar supplemented as described above. DMSO (vehicle control) or the
684 covalent DsbB inhibitor 4,5-dichloro-2-(2-chlorobenzyl)pyridazin-3-one (final concentration
685 of 50 μ M) (Enamine) were added to the medium, as required. 1 μ L of the washed cell
686 suspension was inoculated into the center of a 90 mm diameter agar plate, just below the
687 surface of the semi-solid medium. Plates were incubated at 37 °C in a humidified
688 environment for 16-18 hours and growth halo diameters were measured.

689

690 **AMS labelling.** Bacterial strains to be tested were grown for 18 hours in M63 broth
691 supplemented as described above. DMSO (vehicle control) or the covalent DsbB inhibitor
692 4,5-dichloro-2-(2-chlorobenzyl)pyridazin-3-one (final concentration of 50 μ M) (Enamine)
693 were added to the medium, as required. Cultures were standardized to OD₆₀₀ 2.0 in M63
694 broth, spun at 10,000 \times g for 10 minutes and bacterial pellets lysed by addition of BugBuster
695 Master Mix (Merck Millipore) for 25 minutes at room temperature with gentle agitation.
696 Subsequently, lysates were spun at 10,000 \times g for 10 minutes at 4 °C prior to reaction with 4-
697 acetamido-4'-maleimidyl-stilbene-2,2'-disulfonic acid (AMS) (ThermoFisher Scientific).
698 AMS alkylation was performed by vortexing the lysates in 15 mM AMS, 50 mM Tris-HCl,
699 3% w/v SDS and 3 mM EDTA (pH 8.0) for 30 minutes at 25 °C, followed by incubation at
700 37 °C for 10 minutes. SDS-PAGE analysis and immunoblotting was carried out as described
701 above, except that 12% BisTris NuPAGE gels (ThermoFisher Scientific) and MOPS/SDS
702 running buffer were used. DsbA was detected using a rabbit anti-DsbA primary antibody and
703 an AP-conjugated secondary antibody, as described above.

704

705 **Bacterial growth assays.** To assess the effect of DSB system inhibition of the growth of *E.*
706 *coli*, overnight cultures of the strains to be tested were centrifuged and the pellets were
707 washed three times in M63 broth before transfer to clear-bottomed 96-well microtiter plates
708 (Corning) at approximately 5 \times 10⁷ CFU/well (starting OD₆₀₀ ~ 0.03). M63 broth
709 supplemented as described above was used as a growth medium. DMSO (vehicle control) or
710 the covalent DsbB inhibitor 4,5-dichloro-2-(2-chlorobenzyl)pyridazin-3-one (final
711 concentration of 50 μ M) (Enamine) were added to the medium, as required. Plates were
712 incubated at 37 °C with orbital shaking (amplitude 3 mm, equivalent to ~ 220 RPM) and
713 OD₆₀₀ was measured at 900-second intervals for 18 hours using an Infinite M200 Pro
714 microplate reader (Tecan). The same experimental setup was also used for recording growth
715 curves of *E. coli* strains and their isogenic mutants, except that overnight cultures of the
716 strains to be tested were diluted 1:100 into clear-bottomed 96-well microtiter plates (Corning)
717 (starting OD₆₀₀ ~ 0.01) and that LB was used as the growth medium.

718

719 **Galleria mellonella survival assay.** The wax moth model *Galleria mellonella* was used for *in*
720 *vivo* survival assays (74). Individual *G. mellonella* larvae were randomly allocated to
721 experimental groups; no masking was used. Overnight cultures of the strains to be tested
722 were standardized to OD₆₀₀ 1.0, suspensions were centrifuged and the pellets were washed
723 three times in PBS and serially diluted. 10 μ l of the 1:10 dilution of each bacterial suspension
724 was injected into the last right abdominal proleg of 30 *G. mellonella* larvae per condition; an
725 additional ten larvae were injected with PBS as negative control. Immediately after infection,
726 larvae were injected with 4 μ l of ceftazidime to a final concentration of 7.5 μ g/ml in the last
727 left abdominal proleg. The larvae mortality was monitored for 50 hours. Death was scored
728 when larvae turned black due to melanization, and did not respond to physical stimulation.

729

730 **SEM imaging.** Bacterial strains to be tested were grown for 18 hours in MH broth; the
731 covalent DsbB inhibitor 4,5-dichloro-2-(2-chlorobenzyl)pyridazin-3-one (final concentration
732 of 50 μ M) (Enamine) was added to the medium, as required. Cells were centrifuged, the
733 pellets were washed three times in M63 broth, and cell suspensions were diluted 1:500 into
734 the same medium supplemented as described above; the covalent DsbB inhibitor (final
735 concentration of 50 μ M) and/or antibiotics (final concentrations of 6 μ g/mL and 2 μ g/mL of
736 imipenem and colistin, respectively) were added to the cultures, as required. After 1 hour of
737 incubation as described above, 25 μ l of each culture was spotted onto positively charged
738 glass microscope slides and allowed to air-dry. Cells were then fixed with glutaraldehyde

739 (2.5% v/v in PBS) for 30 min at room temperature and the slide was washed five times in
740 PBS. Subsequently, each sample was dehydrated using increasing concentrations of ethanol
741 (5% v/v, 10% v/v, 20% v/v, 30% v/v, 50% v/v, 70% v/v, 90% v/v (applied three times) and
742 100% v/v), with each wash being carried out by application and immediate removal of the
743 washing solution, before a 7 nm coat of platinum/palladium was applied using a Cressington
744 208 benchtop sputter coater. Images were obtained on a Zeiss Supra 40V Scanning Electron
745 Microscope at 5.00 kV and with 26,000 x magnification.

746
747 **Statistical analysis of experimental data.** The total numbers of performed biological
748 experiments and technical repeats are mentioned in the figure legend of each display item.
749 Biological replication refers to completely independent repetition of an experiment using
750 different biological and chemical materials. Technical replication refers to independent data
751 recordings using the same biological sample. For MIC assays, all recorded values are
752 displayed in the relevant graphs; for MIC assays where three or more biological experiments
753 were performed, the bars indicate the median value, while for assays where two biological
754 experiments were performed the bars indicate the most conservative of the two values (i.e.,
755 for increasing trends, the value representing the smallest increase and for decreasing trends,
756 the value representing the smallest decrease). For all other assays, statistical analysis was
757 performed in GraphPad Prism v8.0.2 using an unpaired T-test with Welch's correction, a
758 one-way ANOVA with correction for multiple comparisons, or a Mantel-Cox logrank test, as
759 appropriate. Statistical significance was defined as $p < 0.05$. Outliers were defined as any
760 technical repeat >2 SD away from the average of the other technical repeats within the same
761 biological experiment. Such data were excluded and all remaining data were included in the
762 analysis. Detailed information for each figure is provided below:
763

764 Figure 2C: unpaired T-test with Welch's correction; $n=3$; 3.621 degrees of freedom, t -
765 value=0.302, $p=0.7792$ (non-significance) (for pDM1 strains); 3.735 degrees of freedom, t -
766 value=0.4677, $p=0.666$ (non-significance) (for pDM1-*bla*_{L2-1} strains); 2.273 degrees of
767 freedom, t -value=5.069, $p=0.0281$ (significance) (for pDM1-*bla*_{GES-1} strains); 2.011 degrees
768 of freedom, t -value=6.825, $p=0.0205$ (significance) (for pDM1-*bla*_{OXA-4} strains); 2.005
769 degrees of freedom, t -value=6.811, $p=0.0208$ (significance) (for pDM1-*bla*_{OXA-10} strains);
770 2.025 degrees of freedom, t -value=5.629, $p=0.0293$ (significance) (for pDM1-*bla*_{OXA-198}
771 strains)

772 Figure 3C: one-way ANOVA with Tukey's multiple comparison test; $n=4$; 24 degrees of
773 freedom; F value=21.00; $p=0.000000000066$ (for pDM1-*mcr-3* strains), $p=0.0004$ (for
774 pDM1-*mcr-4* strains), $p=0.000000000066$ (for pDM1-*mcr-5* strains), $p=0.00066$ (for pDM1-
775 *mcr-8* strains)

776 Figure 5B: one-way ANOVA with Bonferroni's multiple comparison test; $n=3$; 6 degrees of
777 freedom; F value=1878; $p=0.000000002$ (significance)

778 Figure 7C: Mantel-Cox test; $n=30$; $p=<0.0001$ (significance) (*P. aeruginosa* versus *P.*
779 *aeruginosa* *dsbA1*), $p>0.9999$ (non-significance) (*P. aeruginosa* vs *P. aeruginosa* treated
780 with ceftazidime), $p=<0.0001$ (significance) (*P. aeruginosa* treated with ceftazidime versus
781 *P. aeruginosa* *dsbA1*), $p=<0.0001$ (significance) (*P. aeruginosa* *dsbA1* versus *P. aeruginosa*
782 *dsbA1* treated with ceftazidime)

783 Figure 1 - figure supplement 7A(left graph): one-way ANOVA with Bonferroni's multiple
784 comparison test; $n=3$; 6 degrees of freedom; F value=39.22; $p=0.0007$ (significance), $p=0.99$
785 (non-significance)

786 Figure 1 - figure supplement 7B (left graph): one-way ANOVA with Bonferroni's multiple
787 comparison test; $n=3$; 6 degrees of freedom; F value=61.84; $p=0.0002$ (significance), $p=0.99$
788 (non-significance)

789 Figure 1 - figure supplement 7B (right graph): unpaired T-test with Welch's correction, n=3;
790 4 degrees of freedom; t-value=0.1136, p=0.9150 (non-significance)

791 Figure 1 - figure supplement 9A (left graph): one-way ANOVA with Bonferroni's multiple
792 comparison test; n=3; 6 degrees of freedom; F value=261.4; p=0.00000055 (significance),
793 p=0.0639 (non-significance)

794 Figure 1 - figure supplement 9B (left graph): one-way ANOVA with Bonferroni's multiple
795 comparison test; n=3; 6 degrees of freedom; F value=77.49; p=0.0001 (significance),
796 p=0.9999 (non-significance)

797 Figure 1 - figure supplement 9B (right graph): unpaired T-test with Welch's correction, n=3;
798 4 degrees of freedom; t-value=0.02647, p=0.9801 (non-significance)

799

800 **Bioinformatics.** The following bioinformatics analyses were performed in this study. Short
801 scripts and pipelines were written in Perl (version 5.18.2) and executed on macOS Sierra
802 10.12.5.

803

804 **β -lactamase enzymes.** All available protein sequences of β -lactamases were downloaded from
805 <http://www.bldb.eu> (75) (5 August 2021). Sequences were clustered using the ucluster
806 software with a 90% identity threshold and the cluster_fast option (USEARCH v.7.0 (76));
807 the centroid of each cluster was used as a cluster identifier for every sequence. All sequences
808 were searched for the presence of cysteine residues using a Perl script. Proteins with two or
809 more cysteines after the first 30 amino acids of their primary sequence were considered
810 potential substrates of the DSB system for organisms where oxidative protein folding is
811 carried out by DsbA and provided that translocation of the β -lactamase outside the cytoplasm
812 is performed by the Sec system. The first 30 amino acids of each sequence were excluded to
813 avoid considering cysteines that are part of the signal sequence mediating the translocation of
814 these enzymes outside the cytoplasm. The results of the analysis can be found in
815 Supplementary Table 1.

816

817 **MCR enzymes.** *E. coli* MCR-1 (AKF16168.1) was used as a query in a blastp 2.2.28+ (77)
818 search limited to *Proteobacteria* on the NCBI Reference Sequence (RefSeq) proteome
819 database (21 April 2019) (evalue < 10e-5). 17,503 hit sequences were retrieved and clustered
820 using the ucluster software with a 70% identity threshold and the cluster_fast option
821 (USEARCH v.7.0 (76)). All centroid sequences were retrieved and clustered again with a
822 20% identity threshold and the cluster_fast option. Centroid sequences of all clusters
823 comprising more than five sequences (809 sequences retrieved) along with the sequences of
824 the five MCR enzymes tested in this study were aligned using MUSCLE (78). Sequences
825 which were obviously divergent or truncated were manually eliminated and a phylogenetic
826 tree was built from a final alignment comprising 781 sequences using FastTree 2.1.7 with the
827 wag substitution matrix and default parameters (79). The assignment of each protein
828 sequence to a specific group was done using hmmsearch (HMMER v.3.1b2) (80) with
829 Hidden Markov Models built from confirmed sequences of MCR-like and EptA-like proteins.

830

831 **Data availability.** All data generated during this study that support the findings are included
832 in the manuscript or in the Supplementary Information. All materials are available from the
833 corresponding author upon request.

834 **ACKNOWLEDGEMENTS:** We thank J. Rowley for assistance with flow cytometry. SEM
835 imaging was performed at the University of Texas Center for Biomedical Research Support
836 core; we thank M. Mikesh for providing the training for the acquisition of SEM images. We
837 are grateful to IHMA Inc. Schaumburg for the kind gift of the *E. coli* 1144230 isolate, T.
838 Bernhardt for the kind gift of the pCB112 plasmid, and J. Beckwith, F. Alcock and V.
839 Koronakis for the kind gifts of the anti-DsbA, the anti-AcrA and the anti-TolC antibodies,
840 respectively. This study was funded by the MRC Career Development Award
841 MR/M009505/1 (to D.A.I.M.), the institutional BBSRC-DTP studentships BB/M011178/1
842 (to N.K.) and BB/M01116X/1 (to H.L.P.), the BBSRC David Philips Fellowship
843 BB/M02623X/1 (to J.M.A.B.), the ISSF Wellcome Trust grant 105603/Z/14/Z (to G.L.-M.),
844 the Brunel Research Innovation and Enterprise Fund, Innovate UK and British Society for
845 Antimicrobial Chemotherapy grants 2018-11143, 37800 and BSAC-2018-0095, respectively
846 (to R.R.MC) and the Swiss National Science Foundation Postdoc Mobility and Ambizione
847 Fellowships P300PA_167703 and PZ00P3_180142, respectively (to D.G.).
848

849 **AUTHOR CONTRIBUTIONS:** R.C.D.F. and D.A.I.M. designed the research. R.C.D.F.
850 and N.K. performed most of the experiments. D.B. performed colistin MIC assays and
851 prepared samples for MALDI-TOF analysis. P.B. provided genetic tools and advice on *P.*
852 *aeruginosa* molecular biology. A.A.A.A. performed β -lactam MIC assays. L.D. provided
853 laboratory materials and strains. H.E.M., H.L.P. and J.M.A.B. constructed strains and
854 provided advice on RND efflux pump biology and experimental design. G.L.-M. performed
855 MALDI-TOF experiments and analyzed the data. E.M and R.R.MC performed *G. mellonella*
856 survival assays. D.G. performed *in silico* analyses and advised on several aspects of the
857 project. R.C.D.F., N.K. and D.A.I.M. wrote the manuscript with input from all authors.
858 D.A.I.M. directed the project.
859

860 **DECLARATION OF INTERESTS:** The authors declare no competing interests.

861 **TABLES**

862

863 **Table 1.** Overview of the β -lactamase enzymes investigated in this study. Enzymes GES-1, -2
864 and -11 as well as KPC-2 and -3 belong to the same phylogenetic cluster (GES-42 and KPC-
865 44, respectively, see Supplementary Table 1). All other tested enzymes belong to distinct
866 phylogenetic clusters (Supplementary Table 1). The “Cysteine positions” column states the
867 positions of cysteine residues after position 30 and hence, does not include amino acids that
868 would be part of the periplasmic signal sequence. All β -lactamase enzymes except L2-1
869 (shaded in grey; PDB ID: 1O7E) have one disulfide bond. The “Mobile” column refers to the
870 genetic location of the β -lactamase gene; “yes” indicates that the gene of interest is located on
871 a plasmid, while “no” refers to chromosomally-encoded enzymes. All tested enzymes have a
872 broad hydrolytic spectrum and are either Extended Spectrum β -Lactamases (ESBLs) or
873 carbapenemases. The “Inhibition” column refers to classical inhibitor susceptibility i.e.,
874 susceptibility to inhibition by clavulanic acid, tazobactam or sulbactam.

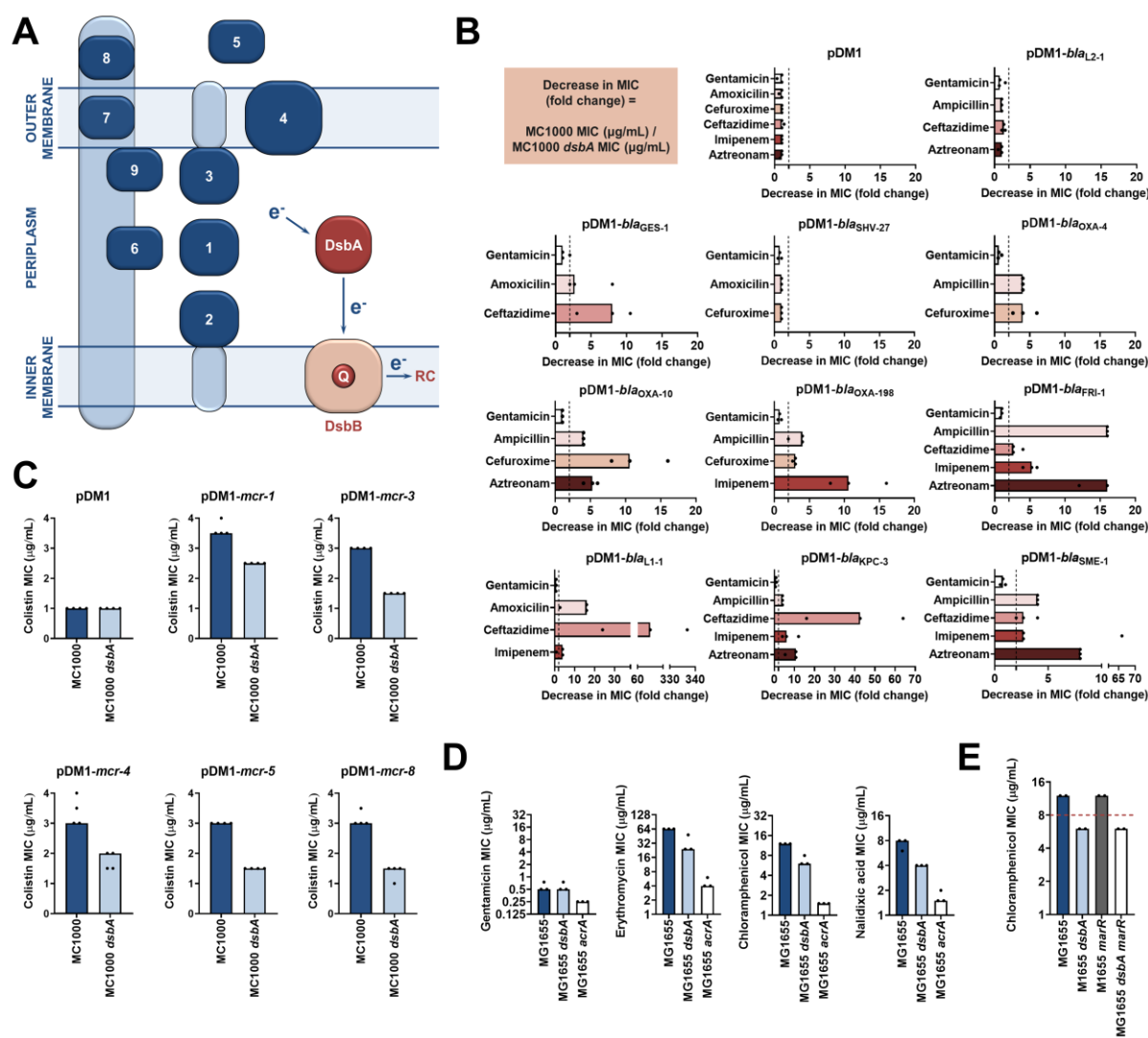
875

876

Enzyme	Ambler class	Cysteine positions	Mobile	Spectrum	Inhibition
L2-1	A	C82 C136 C233	no	ESBL	yes
GES-1	A	C63 C233	yes	ESBL	yes
GES-2	A	C63 C233	yes	ESBL	yes
GES-11	A	C63 C233	yes	Carbapenemase	yes
SHV-27	A	C73 C119	no	ESBL	yes
OXA-4	D	C43 C63	yes	ESBL	yes
OXA-10	D	C44 C51	yes	ESBL	no (81)
OXA-198	D	C116 C119	yes	Carbapenemase	no (82)
FRI-1	A	C68 C238	yes	Carbapenemase	no (83)
L1-1	B3	C239 C267	no	Carbapenemase	no (84)
KPC-2	A	C68 C237	yes	Carbapenemase	no (85)
KPC-3	A	C68 C237	yes	Carbapenemase	no (85)
SME-1	A	C72 C242	no	Carbapenemase	yes

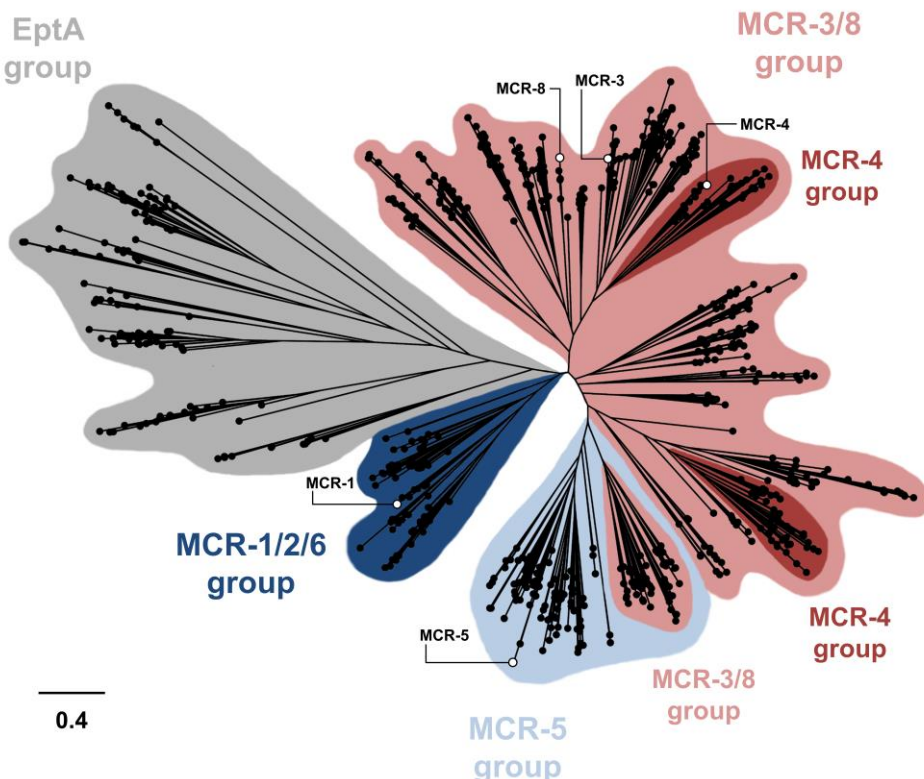
877

878 **FIGURES**
879
880
881



882
883
884
885 **Figure 1. Several antimicrobial resistance mechanisms depend on disulfide bond**
886 **formation.** (A) DsbA introduces disulfide bonds into extracytoplasmic proteins containing
887 two or more cysteine residues. After each round of oxidative protein folding, DsbA is
888 regenerated by the quinone (Q)-containing protein DsbB, which in turn transfers the reducing
889 equivalents to the respiratory chain (RC) (63). DsbA substrates (in dark blue) are distributed
890 throughout the extracytoplasmic space of Gram-negative bacteria. Disulfides are introduced
891 to 1) soluble periplasmic proteins (e.g. alkaline phosphatase, β -lactamases (18)), 2)
892 periplasmic domains of inner-membrane proteins (e.g. LptA-like enzymes (28)), 3)
893 periplasmic domains of outer-membrane proteins (e.g. RcsF (19)), 4) outer-membrane
894 proteins (e.g. OmpA, LptD (19, 25)), 5) secreted proteins (e.g. toxins or enzymes (25)), 6-9)
895 protein components of macromolecular assemblies like secretion systems, pili or flagella (25)
896 (e.g. 6) GspD, 7) EscC, 8) BfpA, 9) FlgI); all examples are *E. coli* proteins with the exception
897 of LptA. (B) β -lactam MIC values for *E. coli* MC1000 expressing diverse disulfide-bond-
898 containing β -lactamases (Ambler classes A, B and D) are substantially reduced in the absence
899 of DsbA (MIC fold changes: >2, fold change of 2 is indicated by the black dotted lines); no

900 effect is observed for SHV-27, which is further discussed in Figure 1 - figure supplement 3.
901 DsbA dependence is conserved within phylogenetic groups (see Figure 1 - figure supplement
902 2). No changes in MIC values are observed for the aminoglycoside antibiotic gentamicin
903 (white bars) confirming that absence of DsbA does not compromise the general ability of this
904 strain to resist antibiotic stress. No changes in MIC values are observed for strains harboring
905 the empty vector control (pDM1) or those expressing the class A β -lactamase L2-1, which
906 contains three cysteines but no disulfide bond (top row). Graphs show MIC fold changes for
907 β -lactamase-expressing *E. coli* MC1000 and its *dsbA* mutant from three biological
908 experiments each conducted as a single technical repeat; the MIC values used to generate this
909 panel are presented in Supplementary Table 2. **(C)** Colistin MIC values for *E. coli* MC1000
910 expressing diverse MCR enzymes (Figure 1 - figure supplement 1) are reduced in the absence
911 of DsbA. Graphs show MIC values ($\mu\text{g/mL}$) from four biological experiments, each
912 conducted in technical quadruplicate, to demonstrate the robustness of the observed effects.
913 Gentamicin control data are presented in Figure 1 - figure supplement 6. **(D)** Deletion of
914 *dsbA* reduces the erythromycin, chloramphenicol and nalidixic acid MIC values for *E. coli*
915 MG1655, but no effects are detected for the non-substrate antibiotic gentamicin. The
916 essential pump component AcrA serves as a positive control. Graphs show MIC values
917 ($\mu\text{g/mL}$) from three biological experiments, each conducted as a single technical repeat. **(E)**
918 Deletion of *dsbA* sensitizes the efflux-active *E. coli* MG1655 strain to chloramphenicol; the
919 data presented in the blue and light blue bars were also used to generate part of panel (D).
920 Sensitization is also observed for the *dsbA* mutant of the deregulated *E. coli* MG1655 *marR*
921 strain (chloramphenicol MIC of 6 $\mu\text{g/mL}$). The graph shows MIC values ($\mu\text{g/ml}$) from 2
922 biological experiments, each conducted as a single technical repeat.

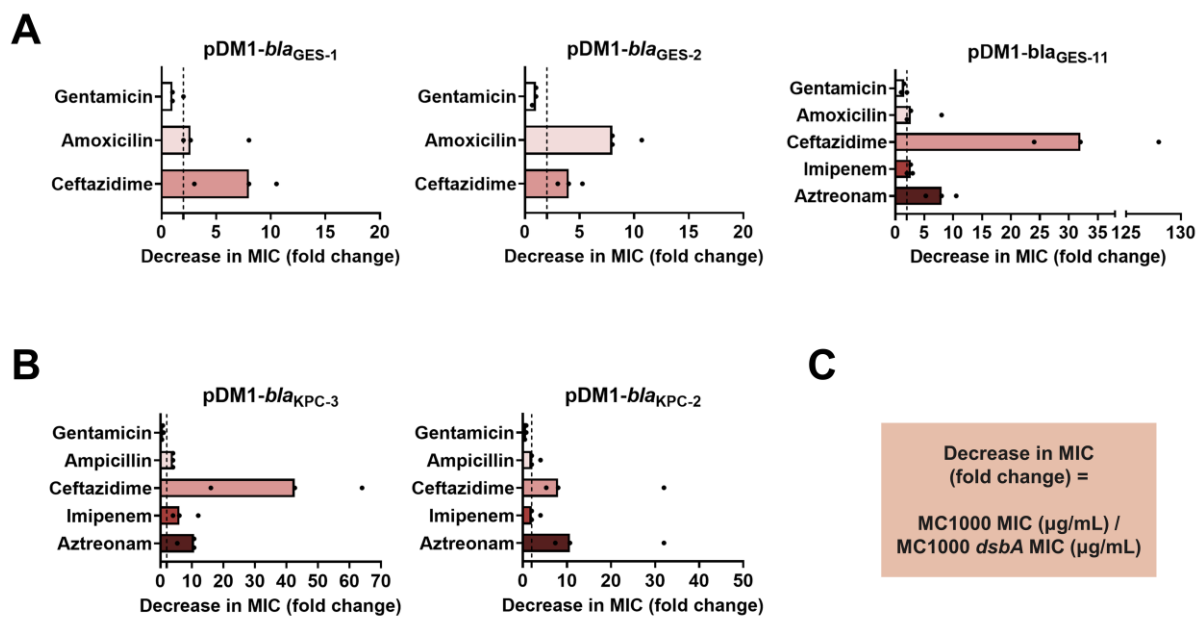


923

924

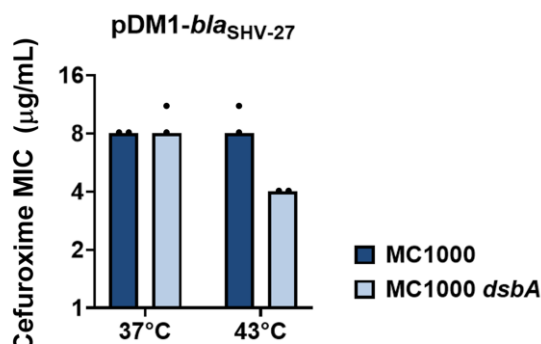
925

926 **Figure 1 - figure supplement 1. Phylogenetic analysis of MCR- and EptA-like enzymes**
927 **found in *Proteobacteria*.** A phylogenetic tree was built based on the alignment of 781
928 sequences from *Proteobacteria*. The assignment of each sequence to a specific group was
929 done using Hidden Markov Models built from confirmed sequences of MCR- and EptA-like
930 proteins; EptA-like enzymes are chromosomally encoded phosphoethanolamine transferases
931 that belong to the same extended protein superfamily as MCR enzymes (86). The different
932 MCR groups are broadly indicated in different colors, however it should be noted that there is
933 significant overlap between groups. Open circles mark the enzymes tested in this study which
934 are distributed throughout the MCR phylogeny.

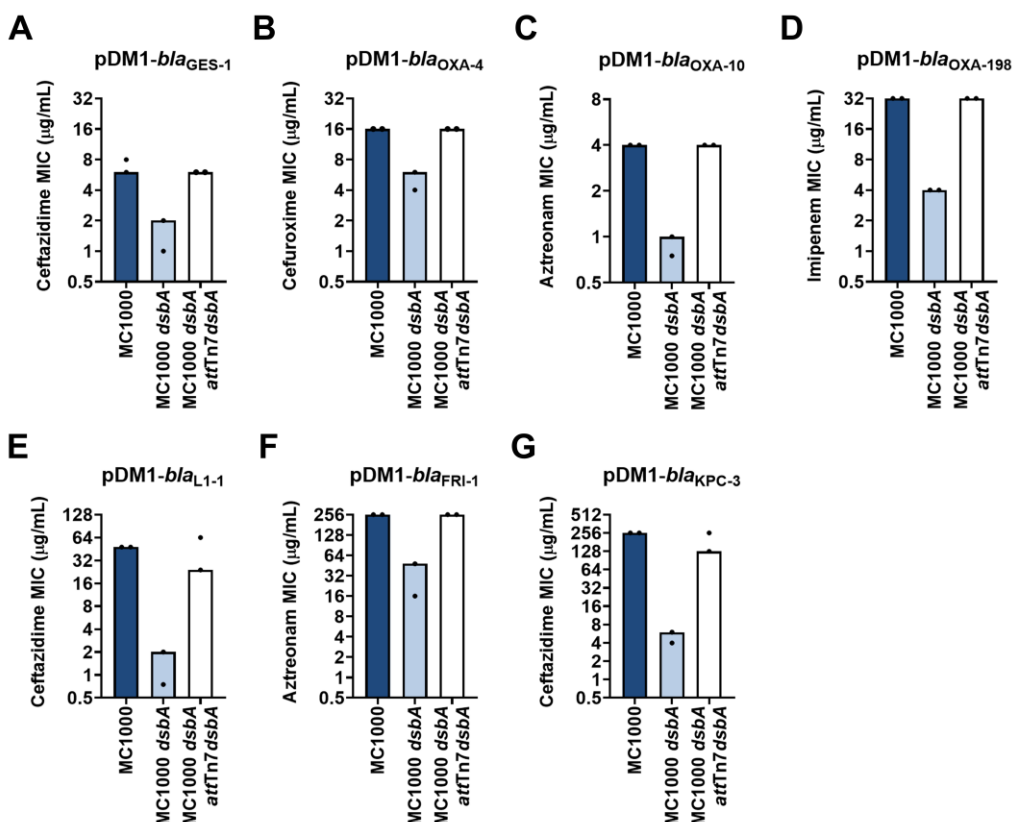


935
936

937 **Figure 1 - figure supplement 2. DsbA dependence is conserved within phylogenetic**
938 **groups of disulfide-bond-containing β -lactamases.** β -lactam MIC values for *E. coli*
939 MC1000 expressing disulfide-bond-containing β -lactamases belonging to the same
940 phylogenetic family (Supplementary Table 1) are substantially reduced in the absence of
941 DsbA for all tested members of each family (MIC fold changes: >2, fold change of 2 is
942 indicated by the black dotted lines). No changes in MIC values are observed for the
943 aminoglycoside antibiotic gentamicin (white bars) confirming that absence of DsbA does not
944 compromise the general ability of this strain to resist antibiotic stress. **(A)** GES β -lactamase
945 enzymes GES-1, -2, and -11; the data for GES-1 presented here are also shown as part of
946 Figure 1B. **(B)** KPC β -lactamase enzymes KPC-3 and -2; the data for KPC-3 presented here
947 are also shown as part of Figure 1B. Graphs show MIC fold changes for β -lactamase-
948 expressing *E. coli* MC1000 and its *dsbA* mutant from three biological experiments each
949 conducted as a single technical repeat; the MIC values used to generate this figure are
950 presented in Supplementary Table 2.

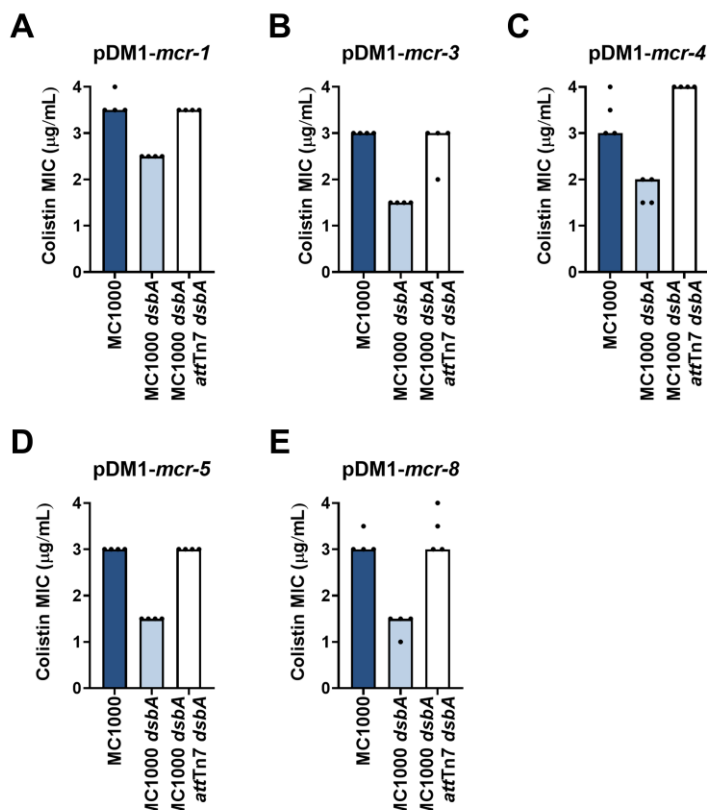


951
952
953 **Figure 1 - figure supplement 3. SHV-27 function is dependent on DsbA at temperatures**
954 **higher than 37 °C.** The ESBL SHV-27 differs from the canonical SHV-1 enzyme by a single
955 amino acid substitution (D156G) (87). At 37 °C deletion of *dsbA* does not affect the
956 cefuroxime MIC for *E. coli* MC1000 harboring pDM1-*bla*_{SHV-27}. However, at 43 °C the
957 cefuroxime MIC for *E. coli* MC1000 *dsbA* harboring pDM1-*bla*_{SHV-27} is notably reduced. The
958 graph shows MIC values (μg/mL) and is representative of three biological experiments, each
959 conducted as a single technical repeat.



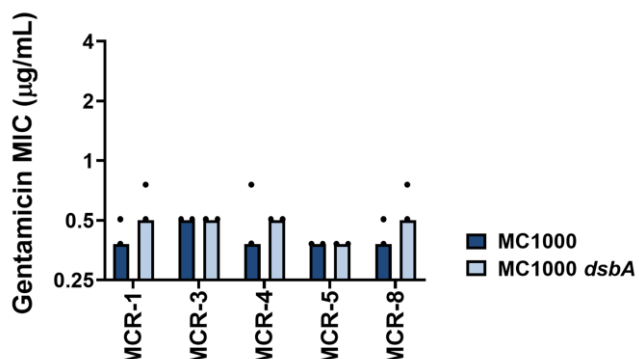
960
961
962
963
964
965
966
967
968
969
970

Figure 1 - figure supplement 4. Complementation of *dsbA* restores the β-lactam MIC values for *E. coli* MC1000 *dsbA* expressing β-lactamases. Re-insertion of *dsbA* at the *attTn7* site of the chromosome restores the β-lactam MIC values for *E. coli* MC1000 *dsbA* harboring (A) pDM1-*bla*_{GES-1} (ceftazidime MIC), (B) pDM1-*bla*_{OXA-4} (cefuroxime MIC), (C) pDM1-*bla*_{OXA-10} (aztreonam MIC), (D) pDM1-*bla*_{OXA-198} (imipenem MIC), (E) pDM1-*bla*_{L1-1} (ceftazidime MIC), (F) pDM1-*bla*_{FRI-1} (aztreonam MIC) and (G) pDM1-*bla*_{KPC-3} (ceftazidime MIC). Graphs show MIC values (μg/mL) from two biological experiments, each conducted as a single technical repeat.



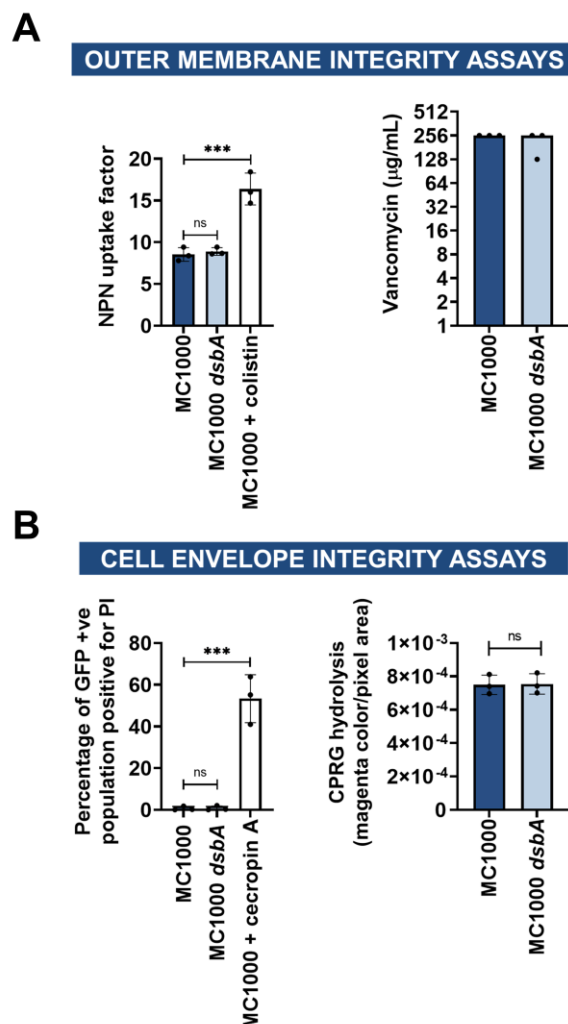
971
972
973
974
975
976
977
978
979

Figure 1 - figure supplement 5. Complementation of *dsbA* restores the colistin MIC values for *E. coli* MC1000 *dsbA* expressing MCR enzymes. Re-insertion of *dsbA* at the *attTn7* site of the chromosome restores the colistin MIC values for *E. coli* MC1000 *dsbA* harboring (A) pDM1-mcr-1 (B) pDM1-mcr-3 (C) pDM1-mcr-4 (D) pDM1-mcr-5 (E) pDM1-mcr-8. Graphs show MIC values ($\mu\text{g/mL}$) from four biological experiments, each conducted in technical quadruplicate, to demonstrate the robustness of the observed effects.



980
981
982
983
984
985
986
987

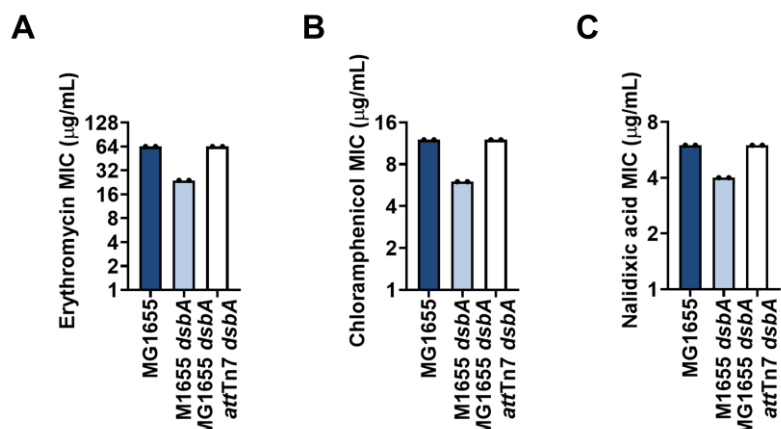
Figure 1 - figure supplement 6. Gentamicin MIC values for *E. coli* MC1000 strains expressing MCR enzymes. Deletion of *dsbA* does not affect the gentamicin MIC values for *E. coli* MC1000 strains expressing MCR enzymes, confirming that absence of DsbA does not compromise the general ability of this strain to resist antibiotic stress. Graphs show MIC values ($\mu\text{g/mL}$) from two biological experiments, each conducted as a single technical repeat.



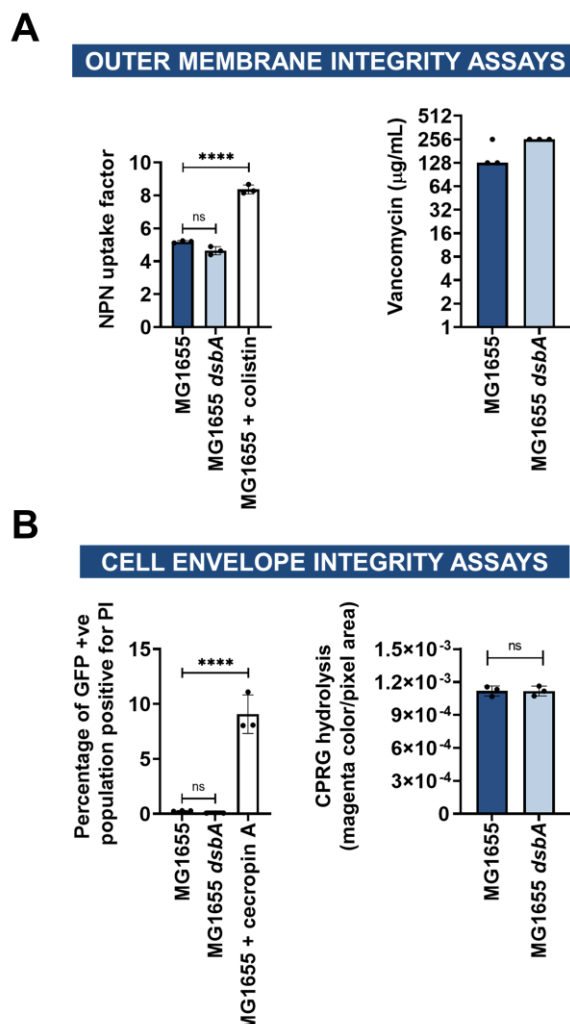
988
989
990

991 **Figure 1 - figure supplement 7. Deletion of *dsbA* has no effect on membrane**
992 **permeability in *E. coli* MC1000. (A) Outer membrane integrity assays. (left)** The bacterial
993 outer membrane acts as a selective permeability barrier to hydrophobic molecules. Deletion
994 of *dsbA* has no effect on the outer membrane integrity of *E. coli* MC1000, as the hydrophobic
995 fluorescent dye NPN crosses the outer membrane of *E. coli* MC1000 and its *dsbA* mutant to
996 the same extent. Conversely, exposure to the outer-membrane-permeabilizing antibiotic
997 colistin results in a significant increase in NPN uptake. **(right)** Outer membrane porins of
998 Gram-negative bacteria are too small to allow the passage of large glycopeptides, such as
999 vancomycin, and therefore increase in vancomycin susceptibility in *E. coli* indicates outer
1000 membrane defects. Deletion of *dsbA* has no effect on the outer membrane integrity of *E. coli*
1001 MC1000, as vancomycin MIC values for both strains do not present major differences. **(B)**
1002 Cell envelope integrity assays. **(left)** PI is a cationic hydrophilic dye that fluoresces upon
1003 intercalation with nucleic acids. Under normal conditions PI freely crosses the outer
1004 membrane but is unable to cross the inner membrane, as no difference in basal PI uptake is seen between
1005 *E. coli* MC1000 and its *dsbA* mutant. Both strains harbor pUltraGFP-GM (71) for superfolder
1006 GFP (sfGFP) expression, and fluorescence was used to distinguish live from dead cells.
1007 Addition of the inner-membrane-permeabilizing antimicrobial peptide cecropin A (88) to *E.*
1008 *coli* MC1000 induces robust inner-membrane permeabilization in the sfGFP-positive
1009 population indicating that the inner membrane becomes compromised. **(right)** CPRG is

1011 excluded from the cytoplasm by the cell envelope, and therefore its hydrolysis by the
1012 cytosolic β -galactosidase is prevented. If both the inner and outer membranes are
1013 compromised, release of β -galactosidase results in CPRG breakdown and the appearance of
1014 red color. The red coloration of *E. coli* MC1000 *dsbA* colonies was comparable to those of
1015 the parent strain, showing that the cell envelope is not compromised in the mutant strain. *E.*
1016 *coli* MC1000 does not express the cytosolic β -galactosidase LacZ (89), so for this assay the
1017 MC1000 strains harbor pCB112 (72), which expresses LacZ exogenously. For NPN and PI
1018 assays, n=3 (each conducted in technical triplicate), graph shows means \pm SD, significance is
1019 indicated by *** = p < 0.001, ns = non-significant. For vancomycin and CPRG hydrolysis
1020 assays, n=3 (each conducted as a single technical triplicate). For CPRG hydrolysis assays,
1021 graph shows means \pm SD, ns = non-significant.



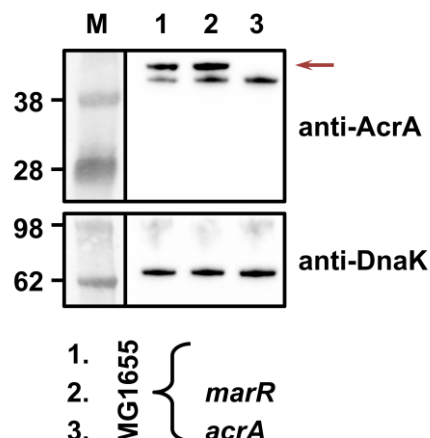
1022
1023
1024
1025 **Figure 1 - figure supplement 8. Complementation of *dsbA* restores efflux-pump**
1026 **substrate MIC values for *E. coli* MG1655 *dsbA*.** Re-insertion of *dsbA* at the *attTn7* site of
1027 the chromosome restores (A) erythromycin, (B) chloramphenicol and (C) nalidixic acid MIC
1028 values for MG1655 *dsbA*. Graphs show MIC values ($\mu\text{g/mL}$) from two biological
1029 experiments, each conducted as a single technical repeat.



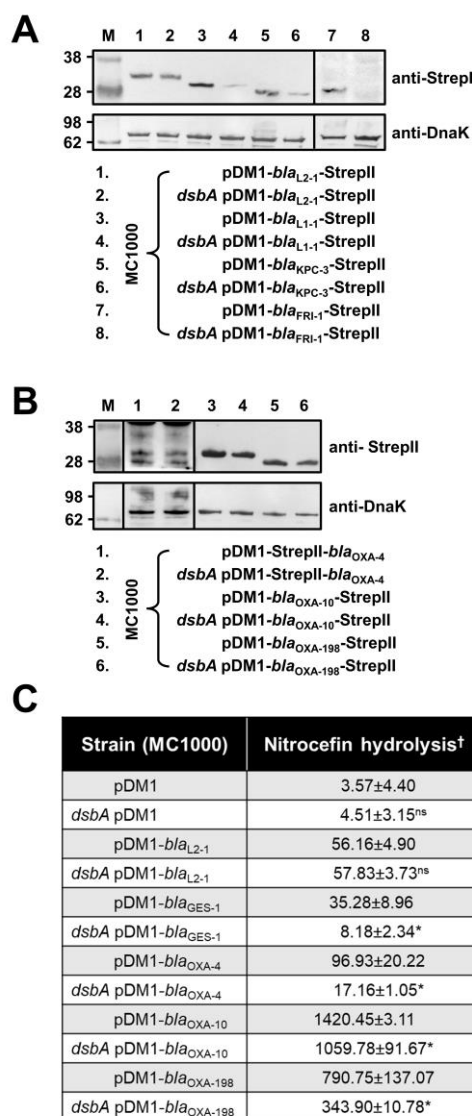
1030
1031
1032

1033 **Figure 1 - figure supplement 9. Deletion of *dsbA* has no effect on membrane**
1034 **permeability in *E. coli* MG1655. (A) Outer membrane integrity assays. (left)** The bacterial
1035 outer membrane acts as a selective permeability barrier to hydrophobic molecules. Deletion
1036 of *dsbA* has no effect on the outer membrane integrity of *E. coli* MG1655, as the hydrophobic
1037 fluorescent dye NPN crosses the outer membrane of *E. coli* MG1655 and its *dsbA* mutant to
1038 the same extent. Conversely, exposure to the outer-membrane-permeabilizing antibiotic
1039 colistin results in a significant increase in NPN uptake. **(right)** Outer membrane porins of
1040 Gram-negative bacteria are too small to allow the passage of large glycopeptides, such as
1041 vancomycin, and therefore increased vancomycin susceptibility in *E. coli* indicates outer
1042 membrane defects. Deletion of *dsbA* has no effect on the outer membrane integrity of *E. coli*
1043 MG1655, as vancomycin MIC values for both strains do not present major differences. **(B)**
1044 Cell envelope integrity assays. **(left)** PI is a cationic hydrophilic dye that fluoresces upon
1045 intercalation with nucleic acids. Under normal conditions PI freely crosses the outer
1046 membrane but is unable to cross the inner membrane. Deletion of *dsbA* does not result in
1047 damage to the bacterial inner membrane, as no difference in basal PI uptake is seen between
1048 *E. coli* MG1655 and its *dsbA* mutant. Both strains harbor pUltraGFP-GM (71) for superfolder
1049 GFP (sfGFP) expression, and fluorescence was used to distinguish live from dead cells.
1050 Addition of the inner-membrane-permeabilizing antimicrobial peptide cecropin A (88) to *E.*
1051 *coli* MG1655 induces robust inner-membrane permeabilization in the sfGFP-positive
1052 population indicating that the inner membrane becomes compromised. **(right)** CPRG is

1053 excluded from the cytoplasm by the cell envelope, and therefore its hydrolysis by the
1054 cytosolic β -galactosidase is prevented. If both the inner and outer membranes are
1055 compromised, release of β -galactosidase results in CPRG breakdown and the appearance of
1056 red color. The red coloration of *E. coli* MG1655 *dsbA* colonies was comparable to those of
1057 the parent strain, showing that the cell envelope is not compromised in the mutant strain. For
1058 NPN and PI assays, n=3 (each conducted in technical triplicate), graph shows means \pm SD,
1059 significance is indicated by *** = p < 0.001, ns = non-significant. For vancomycin and
1060 CPRG hydrolysis assays, n=3 (each conducted as a single technical repeat). For CPRG
1061 hydrolysis assays, graph shows means \pm SD, ns = non-significant.



1062
1063
1064
1065 **Figure 1 - figure supplement 10. Deletion of *marR* results in increased expression of the**
1066 **AcrAB pump (lane 2) compared to the parental strain (lane 1) even though the**
1067 **chloramphenicol MIC for both strains is the same (Figure 1E). *E. coli* MG1655 has an**
1068 **already high level of efflux activity and therefore deletion of *marR* does not result in a drastic**
1069 **change in the observed chloramphenicol MIC value. Expression of the AcrAB pump was**
1070 **assessed using an anti-AcrA primary antibody and an HRP-conjugated secondary antibody.**
1071 ***E. coli* MG1655 *acrA* was used as a negative control for AcrA detection (lane 3); the red**
1072 **arrow indicates the position of the AcrA band. A representative blot from two biological**
1073 **experiments, each conducted as a single technical repeat, is shown; molecular weight markers**
1074 **(M) are shown on the left and DnaK was used as a loading control.**



1075
1076
1077

1078 **Figure 2. β -lactamase enzymes from most classes become unstable in the absence of**
1079 **DsbA.** (A) Protein levels of disulfide-bond-containing Ambler class A and B β -lactamases

1080 are drastically reduced when these enzymes are expressed in *E. coli* MC1000 *dsbA*; the

1081 amount of the control enzyme L2-1 is unaffected. (B) Protein levels of Class D disulfide-

1082 bond-containing β -lactamases are unaffected by the absence of DsbA. OXA-4 is detected as

1083 two bands at ~ 28 kDa. For panels (A) and (B) protein levels of StrepII-tagged β -lactamases

1084 were assessed using a Strep-Tactin-AP conjugate or a Strep-Tactin-HRP conjugate. A

1085 representative blot from three biological experiments, each conducted as a single technical

1086 repeat, is shown; molecular weight markers (M) are on the left, DnaK was used as a loading

1087 control and solid black lines indicate where the membrane was cut. (C) The hydrolytic

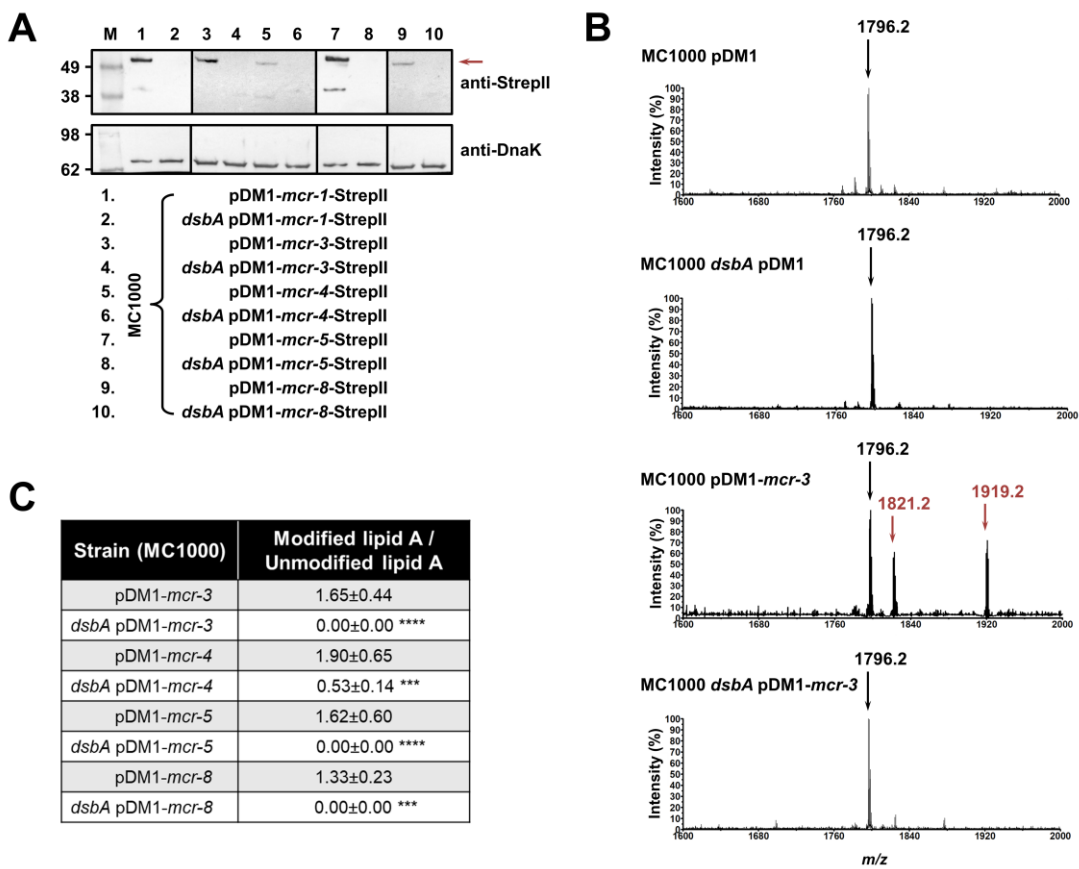
1088 activities of the tested Class D β -lactamases and of the Class A enzyme GES-1, which could

1089 not be detected by immunoblotting, are significantly reduced in the absence of DsbA. The

1090 hydrolytic activities of strains harboring the empty vector or expressing the control enzyme

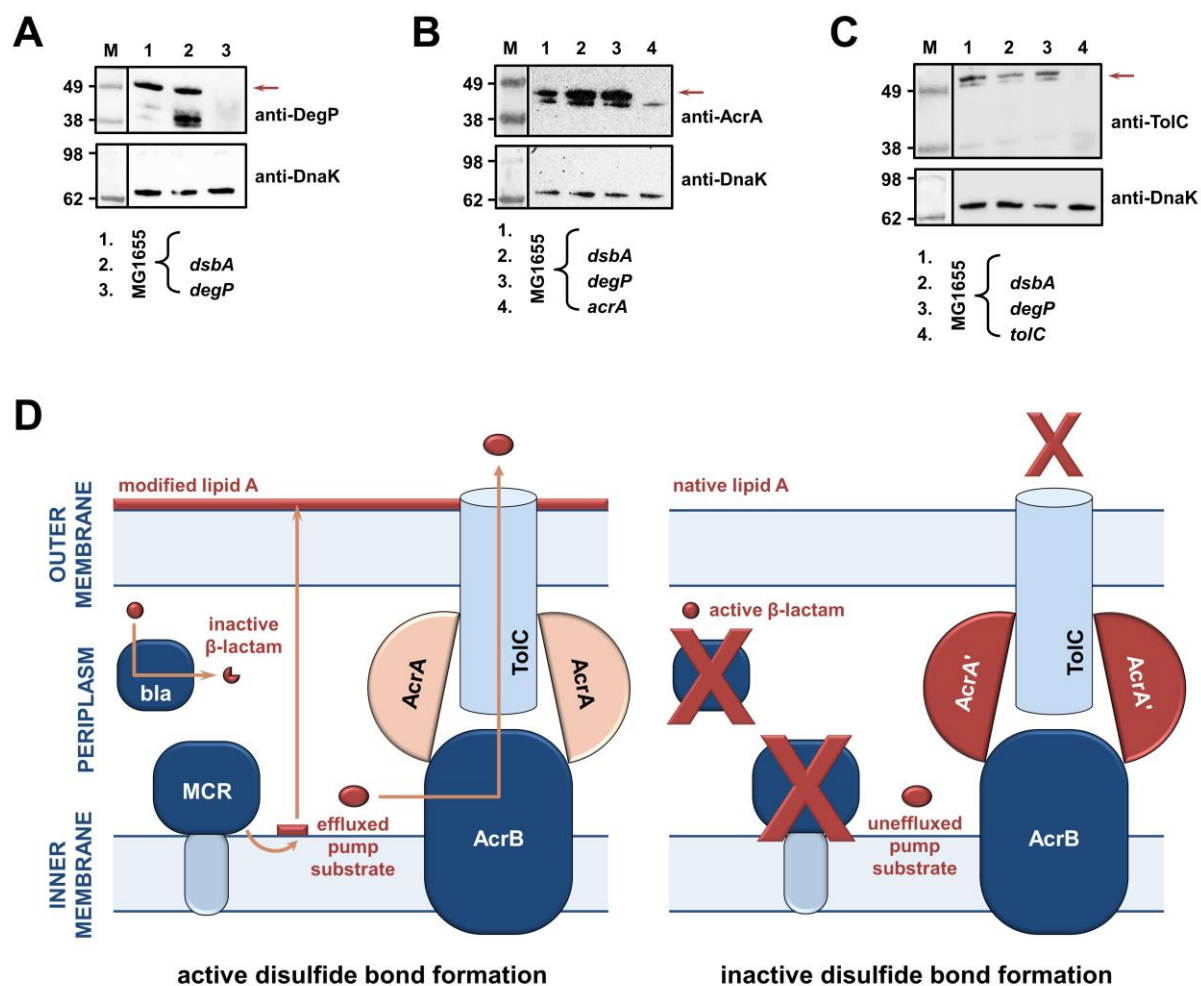
1091 L2-1 show no dependence on DsbA. n=3 (each conducted in technical duplicate), table shows

1092 means \pm SD, significance is indicated by * = p < 0.05, ns = non-significant.



1093
1094
1095

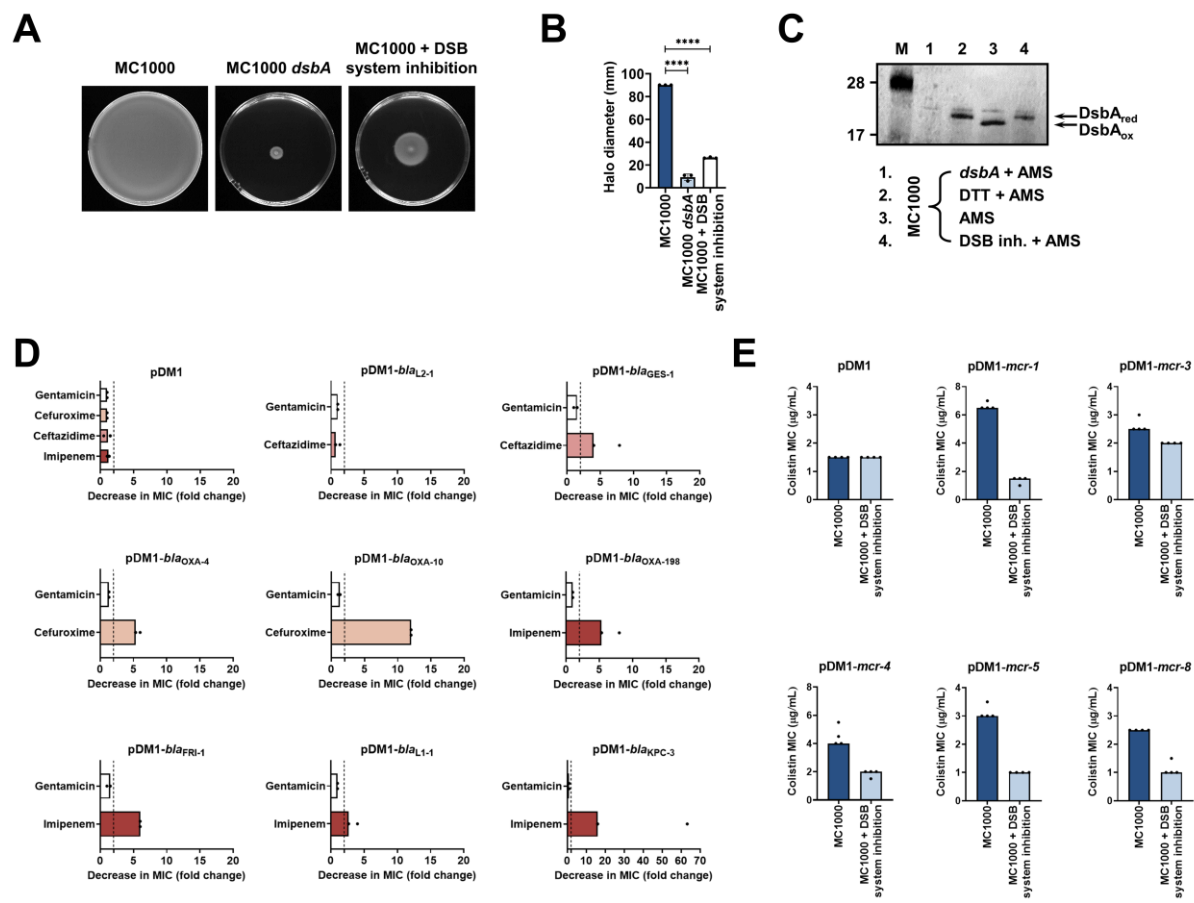
1096 **Figure 3. MCR enzymes become unstable in the absence of DsbA.** (A) The amounts of
1097 MCR proteins are drastically reduced when they are expressed in *E. coli* MC1000 *dsbA*; the
1098 red arrow indicates the position of the MCR-specific bands. Protein levels of StrepII-tagged
1099 MCR enzymes were assessed using a Strep-Tactin-AP conjugate. A representative blot from
1100 three biological experiments, each conducted as a single technical repeat, is shown; molecular
1101 weight markers (M) are on the left, DnaK was used as a loading control and solid black lines
1102 indicate where the membrane was cut. (B) The ability of MCR enzymes to transfer
1103 phoshethanolamine to the lipid A portion of LPS is either entirely abrogated or
1104 significantly reduced in the absence of DsbA. This panel shows representative MALDI-TOF
1105 mass spectra of unmodified and MCR-modified lipid A in the presence and absence of DsbA.
1106 In *E. coli* MC1000 and MC1000 *dsbA* the major peak for native lipid A peak is detected at
1107 m/z 1796.2 (first and second spectrum, respectively). In the presence of MCR enzymes (*E.*
1108 *coli* MC1000 expressing MCR-3 is shown as a representative example), two additional peaks
1109 are observed, at m/z 1821.2 and 1919.2 (third spectrum). For *dsbA* mutants expressing MCR
1110 enzymes (*E. coli* MC1000 *dsbA* expressing MCR-3 is shown), these additional peaks are not
1111 present, whilst the native lipid A peak at m/z 1796.2 remains unchanged (fourth spectrum).
1112 Mass spectra are representative of the data generated from four biological experiments, each
1113 conducted as a technical duplicate. (C) Quantification of the intensities of the lipid A peaks
1114 recorded by MALDI-TOF mass spectrometry for all tested MCR-expressing strains. n=4
1115 (each conducted in technical duplicate), table shows means \pm SD, significance is indicated by
1116 *** = $p < 0.001$ or **** = $p < 0.0001$.



1117
1118
1119

Figure 4. (A, B, C) RND efflux pump function is impaired in the absence of DsbA due to accumulation of unfolded AcrA resulting from insufficient DegP activity. (A) In the absence of DsbA the pool of active DegP is reduced. In *E. coli* MG1655 (lane 1), DegP is detected as a single band, corresponding to the intact active enzyme. In *E. coli* MG1655 *dsbA* (lane 2), an additional lower molecular weight band of equal intensity is present, indicating that DegP is degraded in the absence of its disulfide bond (20, 45). DegP protein levels were assessed using an anti-DegP primary antibody and an HRP-conjugated secondary antibody. *E. coli* MG1655 *degP* was used as a negative control for DegP detection (lane 3); the red arrow indicates the position of intact DegP. **(B)** The RND pump component AcrA accumulates to the same extent in the *E. coli* MG1655 *dsbA* and *degP* strains, indicating that in both strains protein clearance is affected. AcrA protein levels were assessed using an anti-AcrA primary antibody and an HRP-conjugated secondary antibody. *E. coli* MG1655 *acrA* was used as a negative control for AcrA detection; the red arrow indicates the position of the AcrA band. **(C)** TolC, the outer-membrane channel of the AcrAB pump, does not accumulate in a *dsbA* or a *degP* mutant. TolC is not a DegP substrate (47), hence similar TolC protein levels are detected in *E. coli* MG1655 (lane 1) and its *dsbA* (lane 2) and *degP* (lane 3) mutants. TolC protein levels were assessed using an anti-TolC primary antibody and an HRP-conjugated secondary antibody. *E. coli* MG1655 *tolC* was used as a negative control for TolC detection (lane 4); the red arrow indicates the position of the bands originating from TolC. For all panels a representative blot from three biological experiments, each conducted as a single technical repeat, is shown; molecular weight markers (M) are on the left, DnaK was

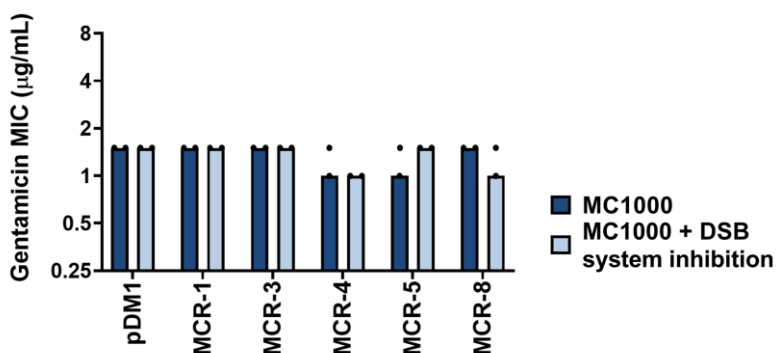
1141 used as a loading control and solid black lines indicate where the membrane was cut. **(D)**
1142 **Impairing disulfide bond formation in the cell envelope simultaneously affects three**
1143 **distinct classes of AMR determinants. (Left)** When DsbA is present, i.e., when disulfide
1144 bond formation occurs, degradation of β -lactam antibiotics by β -lactamases (marked “bla”),
1145 modification of lipid A by MCR proteins and active efflux of RND pump substrates lead to
1146 resistance. The major *E. coli* RND efflux pump AcrAB-TolC is depicted in this schematic as
1147 a characteristic example. **(Right)** In the absence of DsbA, i.e., when the process of disulfide
1148 bond formation is impaired, most cysteine-containing β -lactamases as well as MCR proteins
1149 are unstable and degrade, making bacteria susceptible to β -lactams and colistin, respectively.
1150 Absence of DsbA also affects proteostasis in the cell envelope which results in reduced
1151 clearance of nonfunctional AcrA-like proteins (termed “AcrA” and depicted in dark red
1152 color) by periplasmic proteases. Insufficient clearance of these damaged AcrA components
1153 from the pump complex makes efflux less effective.



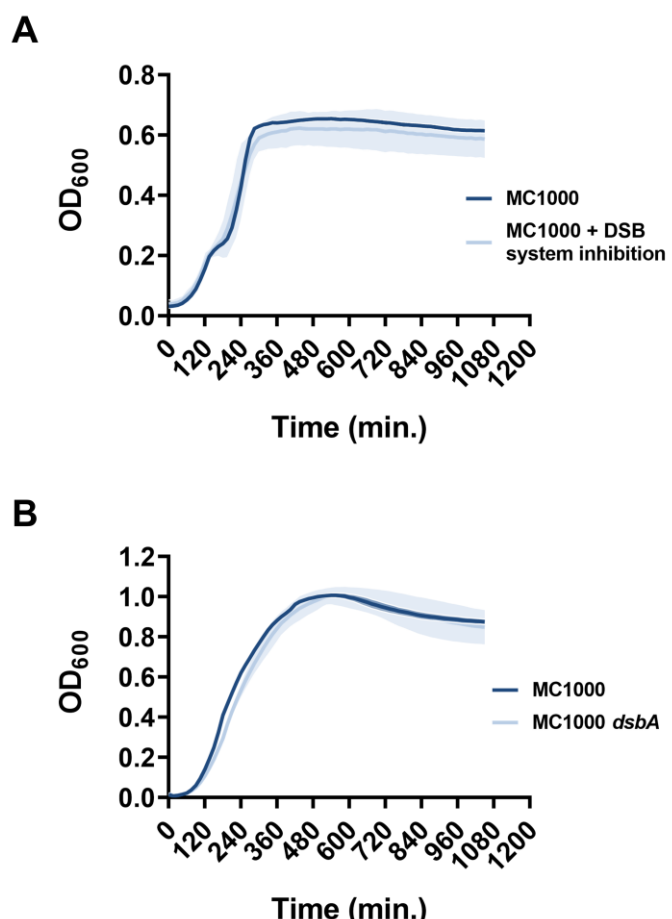
1154
1155
1156

Figure 5. Chemical inhibition of the DSB system impedes DsbA function in *E. coli* MC1000 and phenocopies the β-lactam and colistin MIC changes that were observed using a *dsbA* mutant. (A) Chemical inhibition of the DSB system impedes flagellar motility in *E. coli* MC1000. A functional DSB system is necessary for flagellar motility in *E. coli* because folding of the P-ring component FlgI requires DsbA-mediated disulfide bond formation (52). In the absence of DsbA, or upon addition of a chemical inhibitor of the DSB system, the motility of *E. coli* MC1000 is significantly impeded. Representative images of motility assays are shown. (B) Quantification of the growth halo diameters in the motility assays shown in panel (A). n=3 (each conducted as a single technical repeat), graph shows means ±SD, significance is indicated by **** = p < 0.0001. (C) Chemical inhibition of the DSB system impedes DsbA re-oxidation in *E. coli* MC1000. Addition of the reducing agent DTT to *E. coli* MC1000 bacterial lysates allows the detection of DsbA in its reduced form (DsbA_{red}) during immunoblotting; this redox state of the protein, when labelled with the cysteine-reactive compound AMS, shows a 1 kDa size difference (lane 2) compared to oxidized DsbA as found in AMS-labelled but not reduced lysates of *E. coli* MC1000 (lane 3). Addition of a small-molecule inhibitor of DsbB to growing *E. coli* MC1000 cells also results in accumulation of reduced DsbA (lane 4). *E. coli* MC1000 *dsbA* was used as a negative control for DsbA detection (lane 1). A representative blot from two biological experiments, each conducted as a single technical repeat, is shown; DsbA was visualized using an anti-DsbA primary antibody and an AP-conjugated secondary antibody. Molecular weight markers (M) are shown on the left. (D) MIC experiments using representative β-lactam antibiotics show that chemical inhibition of the DSB system reduces the MIC values for *E. coli* MC1000 expressing disulfide-bond-containing β-lactamases in a similar manner to the deletion of *dsbA* (compare with Figure 1B). Graphs show MIC fold changes (i.e., MC1000

1181 MIC ($\mu\text{g/mL}$) / MC1000 + DSB system inhibitor MIC ($\mu\text{g/mL}$) for β -lactamase-expressing
1182 *E. coli* MC1000 with and without addition of a DSB system inhibitor to the culture medium
1183 from two biological experiments, each conducted as a single technical repeat. Black dotted
1184 lines indicate an MIC fold change of 2. The aminoglycoside antibiotic gentamicin serves as a
1185 control for all strains; gentamicin MIC values (white bars) are unaffected by chemical
1186 inhibition of the DSB system (MIC fold changes: < 2). No changes in MIC values (MIC fold
1187 changes: < 2) are observed for strains harboring the empty vector control (pDM1) or
1188 expressing the class A β -lactamase L2-1, which contains three cysteines but no disulfide
1189 bond (PDB ID: 1O7E) (top row). The MIC values used to generate this panel are presented in
1190 Supplementary Table 2. (E) Colistin MIC experiments show that chemical inhibition of the
1191 DSB system reduces the MIC values for *E. coli* MC1000 expressing MCR enzymes in a
1192 similar manner to the deletion of *dsbA* (compare with Figure 1C). Colistin MIC values for
1193 strains harboring the empty vector control (pDM1) are unaffected by chemical inhibition of
1194 the DSB system. Graphs show MIC values ($\mu\text{g/mL}$) from four biological experiments, each
1195 conducted in technical quadruplicate, to demonstrate the robustness of the observed effects.

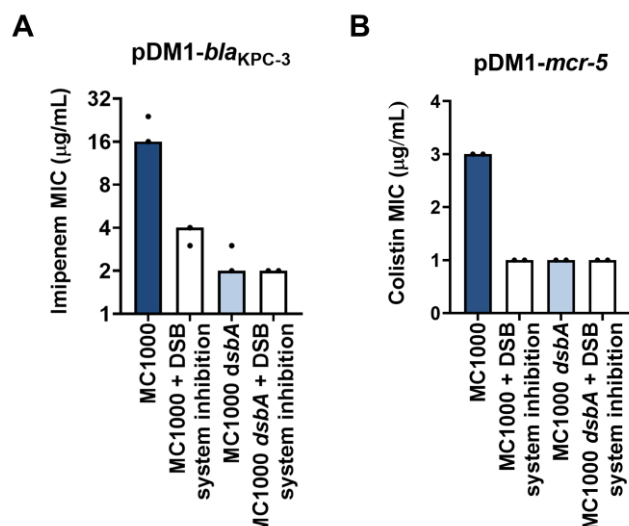


1196
1197
1198
1199 **Figure 5 - figure supplement 1. Gentamicin MIC values for *E. coli* MC1000 strains**
1200 **expressing MCR enzymes.** Chemical inhibition of the DSB system does not affect the
1201 gentamicin MIC values for *E. coli* MC1000 strains expressing MCR enzymes, confirming
1202 that inactivation of DsbA does not compromise the general ability of this strain to resist
1203 antibiotic stress. Graphs show MIC values ($\mu\text{g/mL}$) from two biological experiments, each
1204 conducted as a single technical repeat.



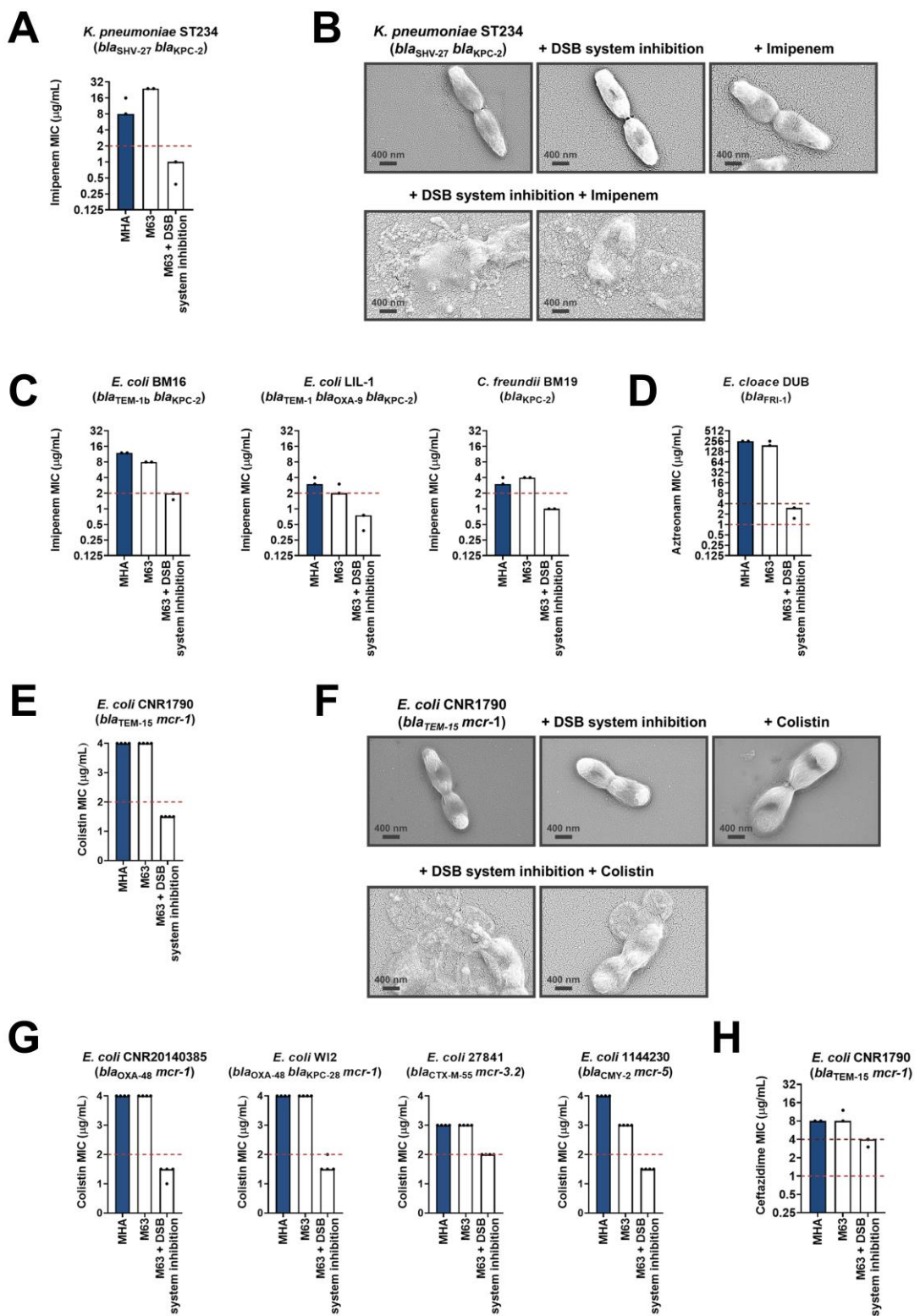
1205
1206
1207

1208 **Figure 5 - figure supplement 2. Chemical inhibition of the DSB system or deletion of**
1209 ***dsbA* does not compromise the growth of *E. coli* MC1000.** Growth curves of (A) *E. coli*
1210 MC1000 with and without chemical inhibition of the DSB system and (B) *E. coli* MC1000
1211 and its *dsbA* mutant show that bacterial growth remains unaffected by the DSB system
1212 inhibitor compound used in this study, or by the absence of DsbA. n=3 (each conducted as a
1213 technical triplicate), solid lines indicate mean values, shaded areas indicate SD.



1214
1215
1216

1217 **Figure 5 - figure supplement 3. Changes in MIC values observed using the DSB system**
1218 **inhibitor are due solely to inhibition of the DSB system. (A)** *E. coli* MC1000 harboring
1219 pDM1-*bla*_{KPC-3} has an imipenem MIC value of 24 $\mu\text{g/mL}$. Upon chemical inhibition of the
1220 DSB system the imipenem MIC for this strain drops to 4 $\mu\text{g/mL}$, and accordingly the
1221 imipenem MIC for *E. coli* MC1000 *dsbA* harboring pDM1-*bla*_{KPC-3} is 2 $\mu\text{g/mL}$. The
1222 imipenem MIC for *E. coli* MC1000 *dsbA* harboring pDM1-*bla*_{KPC-3} when exposed to the
1223 chemical inhibitor of the DSB system is also 2 $\mu\text{g/mL}$, indicating that the chemical
1224 compound used in this study does not have any off-target effects and only affects the function
1225 of the DSB system proteins. **(B)** Chemical inhibition of the DSB system does not lead to any
1226 cumulative effects when tested on an *E. coli* MC1000 strain expressing MCR-5. The colistin
1227 MIC for *E. coli* MC1000 harboring pDM1-*mcr-5* is 3 $\mu\text{g/mL}$ and it drops to 1 $\mu\text{g/mL}$ when
1228 the DSB system is chemically inhibited or *dsbA* is deleted. The same drop in colistin MIC is
1229 observed when the *E. coli* MC1000 *dsbA* strain harboring pDM1-*mcr-5* is exposed to the
1230 chemical inhibitor of the DSB system. Data shown in both panels are from two biological
1231 experiments, each conducted as a single technical repeat.



1232
1233
1234

1235 **Figure 6. Chemical inhibition of the DSB system sensitizes multidrug-resistant clinical**
1236 **isolates to currently available antibiotics.** (A) Addition of a small-molecule inhibitor of

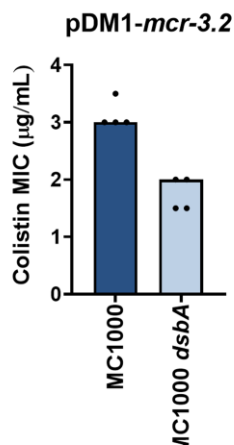
1237 DsbB results in sensitization of a *Klebsiella pneumoniae* clinical isolate to imipenem. (B)

1238 Chemical inhibition of the DSB system in the presence of imipenem (final concentration of 6

1239 μg/mL) results in drastic changes in cell morphology for the *K. pneumoniae* clinical isolate

1240 used in panel (A), while bacteria remain unaffected by single treatments (DSB inhibitor or

1241 imipenem). Images show representative scanning electron micrographs of untreated cells (top
1242 row, left), cells treated with the DSB inhibitor (top row, middle), cells treated with imipenem
1243 (top row, right), and cells treated with both the DSB inhibitor and imipenem (bottom row).
1244 Scale bars are at 400 nm. **(C)** Addition of a small-molecule inhibitor of DsbB results in
1245 sensitization of *E. coli* and *Citrobacter freundii* clinical isolates to imipenem. **(D)** Chemical
1246 inhibition of the DSB system of an *Enterobacter cloacae* clinical isolate harboring *bla*_{FRI-1}
1247 results in reduction of the aztreonam MIC value by over 180 μ g/mL, resulting in intermediate
1248 resistance as defined by EUCAST. For panels (A), (C) and (D) graphs show MIC values
1249 (μ g/ml) from two biological experiments, each conducted as a single technical repeat. **(E)**
1250 Application of the same chemical inhibitor to a colistin-resistant clinical *E. coli* isolate
1251 expressing MCR-1 results in sensitization to colistin. **(F)** Chemical inhibition of the DSB
1252 system in the presence of colistin (final concentration of 2 μ g/mL) results in drastic changes
1253 in cell morphology for the *E. coli* clinical isolate used in panel (E), while bacteria remain
1254 unaffected by single treatments (DSB inhibitor or colistin). Images show representative
1255 scanning electron micrographs of untreated cells (top row, left), cells treated with the DSB
1256 inhibitor (top row, middle), cells treated with colistin (top row, right), and cells treated with
1257 both the DSB inhibitor and colistin (bottom row). Scale bars are at 400 nm. **(G)** Chemical
1258 inhibition of the DSB system results in sensitization of four additional colistin-resistant *E.*
1259 *coli* strains expressing MCR enzymes. For panels (E) and (G) graphs show MIC values
1260 (μ g/mL) from four biological experiments, each conducted in technical quadruplicate, to
1261 demonstrate the robustness of the observed effects. **(H)** Use of the DSB system inhibitor on
1262 the same clinical *E. coli* isolate tested in panel (E), results in intermediate resistance for
1263 ceftazidime as defined by EUCAST. The graph shows MIC values (μ g/ml) from 2 biological
1264 experiments, each conducted as a single technical repeat. For panels (A), (C), (D), (E) and
1265 (G), MIC values determined using Mueller-Hinton agar (MHA) in accordance with the
1266 EUCAST guidelines (dark blue bars) are comparable to the values obtained using defined
1267 media (M63 agar, white bars); use of growth media lacking small-molecule oxidants is
1268 required for the DSB system inhibitor to be effective. For all panels, red dotted lines indicate
1269 the EUCAST clinical breakpoint for each antibiotic, and purple dotted lines indicate the
1270 EUCAST threshold for intermediate resistance.



1271
1272
1273

1274 **Figure 6 - figure supplement 1. Deletion of *dsbA* results in reduced MIC values for *E.*
1275 *coli* MC1000 expressing MCR-3.2.** When cloned into pDM1 and expressed in *E. coli*
1276 MC1000, MCR-3.2 confers colistin resistance as expected (MIC of 3.0-3.5 $\mu\text{g/ml}$). Deletion
1277 of *dsbA* reduces the colistin MIC values for *E. coli* MC1000 expressing MCR-3.2 (MIC \leq 2
1278 $\mu\text{g/mL}$). Graphs show MIC values ($\mu\text{g/mL}$) from four biological experiments, each conducted
1279 in technical quadruplicate, to demonstrate the robustness of the observed effects.

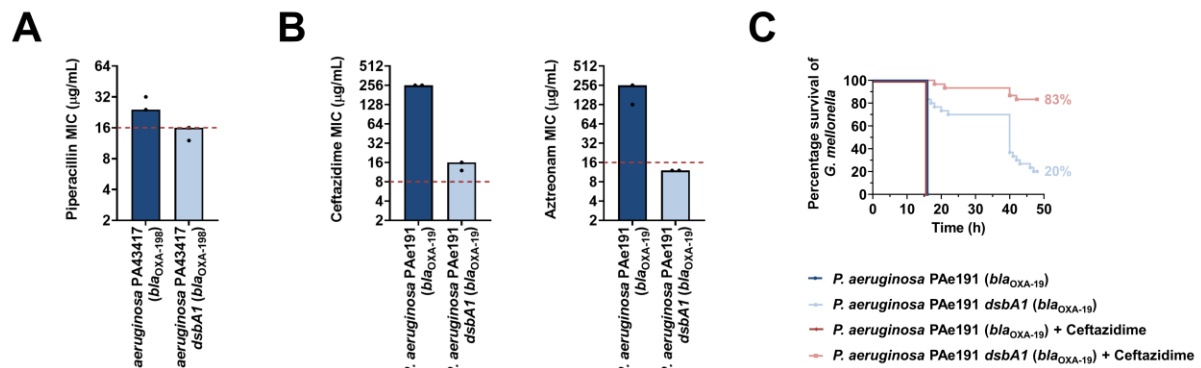


Figure 7. Absence of the principal DsbA analogue (DsbA1) from *P. aeruginosa* clinical isolates expressing OXA enzymes sensitizes them to existing β -lactam antibiotics and dramatically increases the survival of infected *G. mellonella* larvae that undergo antibiotic treatment. (A) Absence of DsbA1 sensitizes the *P. aeruginosa* PA43417 clinical isolate expressing OXA-198 to the first-line antibiotic piperacillin. (B) Absence of DsbA1 sensitizes the *P. aeruginosa* PAe191 clinical isolate expressing OXA-19 to aztreonam and results in reduction of the ceftazidime MIC value by over 220 μ g/mL. For panels (A) and (B) the graphs show MIC values (μ g/ml) from 2 biological experiments, each conducted as a single technical repeat; red dotted lines indicate the EUCAST clinical breakpoint for each antibiotic. (C) 100% of the *G. mellonella* larvae infected with *P. aeruginosa* PAe191 (blue curve) or infected with *P. aeruginosa* PAe191 and treated with 7.5 μ g/mL ceftazidime (red curve) die 18 hours post infection, and only 20% of the larvae infected with *P. aeruginosa* PAe191 *dsbA1* (light blue curve) survive 50 hours post infection. Treatment of larvae infected with *P. aeruginosa* PAe191 *dsbA1* with 7.5 μ g/mL ceftazidime (pink curve) results in 83% survival, 50 hours post infection. The graph shows Kaplan-Meier survival curves of infected *G. mellonella* larvae after different treatment applications; horizontal lines represent the percentage of larvae surviving after application of each treatment at the indicated time point (a total of 30 larvae were used for each curve).

1301 **REFERENCES**

1302

1303 1. Rochford C, Sridhar D, Woods N, Saleh Z, Hartenstein L, Ahlawat H, et al. Global
1304 governance of antimicrobial resistance. *Lancet*. 2018;391(10134):1976-8.

1305 2. Tacconelli E, Carrara E, Savoldi A, Harbarth S, Mendelson M, Monnet DL, et al.
1306 Discovery, research, and development of new antibiotics: the WHO priority list of antibiotic-
1307 resistant bacteria and tuberculosis. *Lancet Infect Dis*. 2018;18(3):318-27.

1308 3. Hart EM, Mitchell AM, Konovalova A, Grabowicz M, Sheng J, Han X, et al. A
1309 small-molecule inhibitor of BamA impervious to efflux and the outer membrane permeability
1310 barrier. *Proc Natl Acad Sci U S A*. 2019;116(43):21748-57.

1311 4. Laws M, Shaaban A, Rahman KM. Antibiotic resistance breakers: current approaches
1312 and future directions. *FEMS Microbiol Rev*. 2019;43(5):490-516.

1313 5. Luther A, Urfer M, Zahn M, Muller M, Wang SY, Mondal M, et al. Chimeric
1314 peptidomimetic antibiotics against Gram-negative bacteria. *Nature*. 2019;576(7787):452-8.

1315 6. Nicolas I, Bordeau V, Bondon A, Baudy-Floc'h M, Felden B. Novel antibiotics
1316 effective against Gram-positive and -negative multi-resistant bacteria with limited resistance.
1317 *PLoS Biol*. 2019;17(7):e3000337.

1318 7. Srinivas N, Jetter P, Ueberbacher BJ, Werneburg M, Zerbe K, Steinmann J, et al.
1319 Peptidomimetic antibiotics target outer-membrane biogenesis in *Pseudomonas aeruginosa*.
1320 *Science*. 2010;327(5968):1010-3.

1321 8. Bush K. Past and present perspectives on b-lactamases. *Antimicrob Agents
1322 Chemother*. 2018;62(10).

1323 9. Meletis G. Carbapenem resistance: overview of the problem and future perspectives.
1324 *Ther Adv Infect Dis*. 2016;3(1):15-21.

1325 10. Versporten A, Zarb P, Caniaux I, Gros MF, Drapier N, Miller M, et al. Antimicrobial
1326 consumption and resistance in adult hospital inpatients in 53 countries: results of an internet-
1327 based global point prevalence survey. *Lancet Glob Health*. 2018;6(6):e619-e29.

1328 11. Li J, Nation RL, Turnidge JD, Milne RW, Coulthard K, Rayner CR, et al. Colistin:
1329 the re-emerging antibiotic for multidrug-resistant Gram-negative bacterial infections. *Lancet
1330 Infect Dis*. 2006;6(9):589-601.

1331 12. Poirel L, Jayol A, Nordmann P. Polymyxins: antibacterial activity, susceptibility
1332 testing, and resistance mechanisms encoded by plasmids or chromosomes. *Clin Microbiol Rev*.
1333 2017;30(2):557-96.

1334 13. Sun J, Zhang H, Liu YH, Feng Y. Towards understanding MCR-like colistin
1335 resistance. *Trends Microbiol*. 2018;26(9):794-808.

1336 14. Blair JMA, Richmond GE, Piddock LJV. Multidrug efflux pumps in Gram-negative
1337 bacteria and their role in antibiotic resistance. *Future Microbiol*. 2014;9(10):1165-77.

1338 15. Cox G, Wright GD. Intrinsic antibiotic resistance: mechanisms, origins, challenges
1339 and solutions. *Int J Med Microbiol*. 2013;303(6-7):287-92.

1340 16. Goemans C, Denoncin K, Collet JF. Folding mechanisms of periplasmic proteins.
1341 *Biochim Biophys Acta*. 2014;1843(8):1517-28.

1342 17. Heras B, Kurz M, Shouldice SR, Martin JL. The name's bond.....disulfide bond. *Curr
1343 Opin Struct Biol*. 2007;17(6):691-8.

1344 18. Bardwell JC, McGovern K, Beckwith J. Identification of a protein required for
1345 disulfide bond formation *in vivo*. *Cell*. 1991;67(3):581-9.

1346 19. Denoncin K, Collet JF. Disulfide bond formation in the bacterial periplasm: major
1347 achievements and challenges ahead. *Antioxid. Redox Signal.* 2013;19(1):63-71.

1348 20. Hiniker A, Bardwell JC. *In vivo* substrate specificity of periplasmic disulfide
1349 oxidoreductases. *J. Biol. Chem.* 2004;279(13):12967-73.

1350 21. Kadokura H, Tian H, Zander T, Bardwell JC, Beckwith J. Snapshots of DsbA in
1351 action: detection of proteins in the process of oxidative folding. *Science*.
1352 2004;303(5657):534-7.

1353 22. Martin JL, Bardwell JC, Kuriyan J. Crystal structure of the DsbA protein required for
1354 disulphide bond formation *in vivo*. *Nature*. 1993;365(6445):464-8.

1355 23. Dutton RJ, Boyd D, Berkmen M, Beckwith J. Bacterial species exhibit diversity in
1356 their mechanisms and capacity for protein disulfide bond formation. *Proc. Natl. Acad. Sci.*
1357 U.S.A. 2008;105(33):11933-8.

1358 24. Vertommen D, Depuydt M, Pan J, Leverrier P, Knoops L, Szikora JP, et al. The
1359 disulphide isomerase DsbC cooperates with the oxidase DsbA in a DsbD-independent
1360 manner. *Mol. Microbiol.* 2008;67(2):336-49.

1361 25. Heras B, Shouldice SR, Totsika M, Scanlon MJ, Schembri MA, Martin JL. DSB
1362 proteins and bacterial pathogenicity. *Nat. Rev. Microbiol.* 2009;7(3):215-25.

1363 26. Landeta C, Boyd D, Beckwith J. Disulfide bond formation in prokaryotes. *Nat.*
1364 *Microbiol.* 2018;3(3):270-80.

1365 27. Heras B, Scanlon MJ, Martin JL. Targeting virulence not viability in the search for
1366 future antibacterials. *Br. J. Clin. Pharmacol.* 2014;79(2):208-15.

1367 28. Piek S, Wang Z, Ganguly J, Lakey AM, Bartley SN, Mowlaboccus S, et al. The role
1368 of oxidoreductases in determining the function of the neisserial lipid A phosphoethanolamine
1369 transferase required for resistance to polymyxin. *PLoS One*. 2014;9(9):e106513.

1370 29. Schultz SC, Dalbadie-McFarland G, Neitzel JJ, Richards JH. Stability of wild-type
1371 and mutant RTEM-1 β -lactamases: effect of the disulfide bond. *Proteins*. 1987;2(4):290-7.

1372 30. Nation RL, Garonzik SM, Li J, Thamlikitkul V, Giamarellos-Bourboulis EJ, Paterson
1373 DL, et al. Updated US and European dose recommendations for intravenous colistin: how do
1374 they perform? *Clin. Infect. Dis.* 2016;62(5):552-8.

1375 31. Plachouras D, Karvanen M, Friberg LE, Papadomichelakis E, Antoniadou A,
1376 Tsangaris I, et al. Population pharmacokinetic analysis of colistin methanesulfonate and
1377 colistin after intravenous administration in critically ill patients with infections caused by
1378 Gram-negative bacteria. *Antimicrob. Agents Chemother.* 2009;53(8):3430-6.

1379 32. Nation RL, Rigatto MHP, Falci DR, Zavascki AP. Polymyxin acute kidney injury:
1380 dosing and other strategies to reduce toxicity. *Antibiotics*. 2019;8(1).

1381 33. Wang Z, Fan G, Hryc CF, Blaza JN, Serysheva, II, Schmid MF, et al. An allosteric
1382 transport mechanism for the AcrAB-TolC multidrug efflux pump. *eLife*. 2017;6.

1383 34. Nikaido H. Multidrug efflux pumps of Gram-negative bacteria. *J. Bacteriol.*
1384 1996;178(20):5853-9.

1385 35. Aires JR, Nikaido H. Aminoglycosides are captured from both periplasm and
1386 cytoplasm by the AcrD multidrug efflux transporter of *Escherichia coli*. *J. Bacteriol.*
1387 2005;187(6):1923-9.

1388 36. Rosenberg EY, Ma D, Nikaido H. AcrD of *Escherichia coli* is an aminoglycoside
1389 efflux pump. *J. Bacteriol.* 2000;182(6):1754-6.

1390 37. Yamasaki S, Nagasawa S, Hayashi-Nishino M, Yamaguchi A, Nishino K. AcrA
1391 dependency of the AcrD efflux pump in *Salmonella enterica* serovar Typhimurium. *J.*
1392 *Antibiot.* 2011;64(6):433-7.

1393 38. Ariza RR, Cohen SP, Bachhawat N, Levy SB, Demple B. Repressor mutations in the
1394 *marRAB* operon that activate oxidative stress genes and multiple antibiotic resistance in
1395 *Escherichia coli*. *J. Bacteriol.* 1994;176(1):143-8.

1396 39. Okusu H, Ma D, Nikaido H. AcrAB efflux pump plays a major role in the antibiotic
1397 resistance phenotype of *Escherichia coli* multiple-antibiotic-resistance (Mar) mutants. *J.*
1398 *Bacteriol.* 1996;178(1):306-8.

1399 40. Keeney D, Ruzin A, McAleese F, Murphy E, Bradford PA. MarA-mediated
1400 overexpression of the AcrAB efflux pump results in decreased susceptibility to tigecycline in
1401 *Escherichia coli*. *J. Antimicrob. Chemother.* 2008;61(1):46-53.

1402 41. Alonso-Caballero A, Schonfelder J, Poly S, Corsetti F, De Sancho D, Artacho E, et al.
1403 Mechanical architecture and folding of *E. coli* type 1 pilus domains. *Nat. Commun.*
1404 2018;9(1):2758.

1405 42. Zheng WD, Quan H, Song JL, Yang SL, Wang CC. Does DsbA have chaperone-like
1406 activity? *Arch. Biochem. Biophys.* 1997;337(2):326-31.

1407 43. Doret L, Bonnin RA, Pennisi I, Gauthier L, Jousset AB, Dabos L, et al. Rapid
1408 detection and discrimination of chromosome- and MCR-plasmid-mediated resistance to
1409 polymyxins by MALDI-TOF MS in *Escherichia coli*: the MALDIxin test. *J. Antimicrob.*
1410 *Chemother.* 2018;73(12):3359-67.

1411 44. Clausen T, Southan C, Ehrmann M. The HtrA family of proteases: implications for
1412 protein composition and cell fate. *Mol. Cell.* 2002;10(3):443-55.

1413 45. Skorko-Glonek J, Zurawa D, Tanfani F, Scire A, Wawrzynow A, Narkiewicz J, et al.
1414 The N-terminal region of HtrA heat shock protease from *Escherichia coli* is essential for
1415 stabilization of HtrA primary structure and maintaining of its oligomeric structure. *Biochim.*
1416 *Biophys. Acta.* 2003;1649(2):171-82.

1417 46. Gerken H, Misra R. Genetic evidence for functional interactions between TolC and
1418 AcrA proteins of a major antibiotic efflux pump of *Escherichia coli*. *Mol. Microbiol.*
1419 2004;54(3):620-31.

1420 47. Werner J, Augustus AM, Misra R. Assembly of TolC, a structurally unique and
1421 multifunctional outer membrane protein of *Escherichia coli* k-12. *J. Bacteriol.*
1422 2003;185(22):6540-7.

1423 48. Duprez W, Premkumar L, Halili MA, Lindahl F, Reid RC, Fairlie DP, et al. Peptide
1424 inhibitors of the *Escherichia coli* DsbA oxidative machinery essential for bacterial virulence.
1425 *J. Med. Chem.* 2015;58(2):577-87.

1426 49. Totsika M, Vagenas D, Paxman JJ, Wang G, Dhouib R, Sharma P, et al. Inhibition of
1427 diverse DsbA enzymes in multi-DsbA encoding pathogens. *Antioxid. Redox Signal.*
1428 2018;29(7):653-66.

1429 50. Landeta C, Blazyk JL, Hatahet F, Meehan BM, Eser M, Myrick A, et al. Compounds
1430 targeting disulfide bond forming enzyme DsbB of Gram-negative bacteria. *Nat. Chem. Biol.*
1431 2015;11(4):292-8.

1432 51. Halili MA, Bachu P, Lindahl F, Bechara C, Mohanty B, Reid RC, et al. Small
1433 molecule inhibitors of disulfide bond formation by the bacterial DsbA-DsbB dual enzyme
1434 system. *ACS Chem. Biol.* 2015;10(4):957-64.

1435 52. Dailey FE, Berg HC. Mutants in disulfide bond formation that disrupt flagellar
1436 assembly in *Escherichia coli*. *Proc. Natl. Acad. Sci. U.S.A.* 1993;90(3):1043-7.

1437 53. Hizukuri Y, Yakushi T, Kawagishi I, Homma M. Role of the intramolecular disulfide
1438 bond in FlgI, the flagellar P-ring component of *Escherichia coli*. *J. Bacteriol.*
1439 2006;188(12):4190-7.

1440 54. Kishigami S, Akiyama Y, Ito K. Redox states of DsbA in the periplasm of
1441 *Escherichia coli*. *FEBS Lett.* 1995;364(1):55-8.

1442 55. Arts IS, Ball G, Leverrier P, Garvis S, Nicolaes V, Vertommen D, et al. Dissecting
1443 the machinery that introduces disulfide bonds in *Pseudomonas aeruginosa*. *mBio.* 2013;4(6).

1444 56. Mugnier P, Casin I, Bouthors AT, Collatz E. Novel OXA-10-derived extended-
1445 spectrum beta-lactamases selected *in vivo* or *in vitro*. *Antimicrob. Agents Chemother.*
1446 1998;42(12):3113-6.

1447 57. Landeta C, McPartland L, Tran NQ, Meehan BM, Zhang Y, Tanweer Z, et al.
1448 Inhibition of *Pseudomonas aeruginosa* and *Mycobacterium tuberculosis* disulfide bond
1449 forming enzymes. *Mol. Microbiol.* 2019;111(4):918-37.

1450 58. Zhou YL, Wang JF, Guo Y, Liu XQ, Liu SL, Niu XD, et al. Discovery of a potential
1451 MCR-1 inhibitor that reverses polymyxin activity against clinical *mcr-1*-positive
1452 Enterobacteriaceae. *J. Infect.* 2019;78(5):364-72.

1453 59. Sun H, Zhang Q, Wang R, Wang H, Wong YT, Wang M, et al. Resensitizing
1454 carbapenem- and colistin-resistant bacteria to antibiotics using auranofin. *Nat. Commun.*
1455 2020;11(1):5263.

1456 60. Minrovic BM, Hubble VB, Barker WT, Jania LA, Melander RJ, Koller BH, et al.
1457 Second-generation tryptamine derivatives potently sensitize colistin resistant bacteria to
1458 colistin. *ACS Med. Chem. Lett.* 2019;10(5):828-33.

1459 61. Zimmerman SM, Lafontaine AJ, Herrera CM, McLean AB, Trent MS. A whole-cell
1460 screen identifies small bioactives that synergize with polymyxin and exhibit antimicrobial
1461 activities against multidrug-resistant bacteria. *Antimicrob. Agents Chemother.* 2020;64(3).

1462 62. Sharma A, Gupta VK, Pathania R. Efflux pump inhibitors for bacterial pathogens:
1463 From bench to bedside. *Indian J. Med. Res.* 2019;149(2):129-45.

1464 63. Kadokura H, Katzen F, Beckwith J. Protein disulfide bond formation in prokaryotes.
1465 *Annu. Rev. Biochem.* 2003;72:111-35.

1466 64. Wilmaerts D, Dewachter L, De Loose PJ, Bollen C, Verstraeten N, Michiels J. HokB
1467 monomerization and membrane repolarization control persister awakening. *Mol. Cell.*
1468 2019;75(5):1031-42.

1469 65. Chang AC, Cohen SN. Construction and characterization of amplifiable multicopy
1470 DNA cloning vehicles derived from the P15A cryptic miniplasmid. *J. Bacteriol.*
1471 1978;134(3):1141-56.

1472 66. Kim J, Webb AM, Kershner JP, Blaskowski S, Copley SD. A versatile and highly
1473 efficient method for scarless genome editing in *Escherichia coli* and *Salmonella enterica*.
1474 *BMC Biotechnol.* 2014;14:84.

1475 67. McKenzie GJ, Craig NL. Fast, easy and efficient: site-specific insertion of transgenes
1476 into enterobacterial chromosomes using Tn7 without need for selection of the insertion event.
1477 *BMC Microbiol.* 2006;6:39.

1478 68. Vasseur P, Vallet-Gely I, Soscia C, Genin S, Filloux A. The *pel* genes of the
1479 *Pseudomonas aeruginosa* PAK strain are involved at early and late stages of biofilm
1480 formation. *Microbiology*. 2005;151:985-97.

1481 69. Kaniga K, Delor I, Cornelis GR. A wide-host-range suicide vector for improving
1482 reverse genetics in Gram-negative bacteria: inactivation of the *blaA* gene of *Yersinia*
1483 *enterocolitica*. *Gene*. 1991;109(1):137-41.

1484 70. Helander IM, Mattila-Sandholm T. Fluorometric assessment of Gram-negative
1485 bacterial permeabilization. *J. Appl. Microbiol.* 2000;88(2):213-9.

1486 71. Mavridou DA, Gonzalez D, Clements A, Foster KR. The pUltra plasmid series: a
1487 robust and flexible tool for fluorescent labeling of *Enterobacteria*. *Plasmid*. 2016;87-88:65-
1488 71.

1489 72. Paradis-Bleau C, Kritikos G, Orlova K, Typas A, Bernhardt TG. A genome-wide
1490 screen for bacterial envelope biogenesis mutants identifies a novel factor involved in cell wall
1491 precursor metabolism. *PLoS Genet.* 2014;10(1):e1004056.

1492 73. Larrouy-Maumus G, Clements A, Filloux A, McCarthy RR, Mostowy S. Direct
1493 detection of lipid A on intact Gram-negative bacteria by MALDI-TOF mass spectrometry. *J.*
1494 *Microbiol. Methods*. 2016;120:68-71.

1495 74. McCarthy RR, Mazon-Moya MJ, Moscoso JA, Hao Y, Lam JS, Bordi C, et al. Cyclic-
1496 di-GMP regulates lipopolysaccharide modification and contributes to *Pseudomonas*
1497 *aeruginosa* immune evasion. *Nat. Microbiol.* 2017;2:17027.

1498 75. Naas T, Oueslati S, Bonnin RA, Dabos ML, Zavala A, Dortet L, et al. B-lactamase
1499 database (BLDB) - structure and function. *J. Enzyme Inhib. Med. Chem.* 2017;32(1):917-9.

1500 76. Edgar RC. Search and clustering orders of magnitude faster than BLAST.
1501 *Bioinformatics*. 2010;26(19):2460-1.

1502 77. Altschul SF, Gish W, Miller W, Myers EW, Lipman DJ. Basic local alignment search
1503 tool. *J. Mol. Biol.* 1990;215(3):403-10.

1504 78. Edgar RC. MUSCLE: multiple sequence alignment with high accuracy and high
1505 throughput. *Nucleic acids Res.* 2004;32(5):1792-7.

1506 79. Price MN, Dehal PS, Arkin AP. FastTree 2 - approximately maximum-likelihood
1507 trees for large alignments. *PloS One*. 2010;5(3):e9490.

1508 80. Finn RD, Clements J, Arndt W, Miller BL, Wheeler TJ, Schreiber F, et al. HMMER
1509 web server: 2015 update. *Nucleic acids Res.* 2015;43(W1):W30-8.

1510 81. Aubert D, Poirel L, Ali AB, Goldstein FW, Nordmann P. OXA-35 is an OXA-10-
1511 related b-lactamase from *Pseudomonas aeruginosa*. *J. Antimicrob. Chemother.*
1512 2001;48(5):717-21.

1513 82. El Garch F, Bogaerts P, Bebrone C, Galleni M, Glupczynski Y. OXA-198, an
1514 acquired carbapenem-hydrolyzing class D β -lactamase from *Pseudomonas aeruginosa*.
1515 *Antimicrob. Agents Chemother.* 2011;55(10):4828-33.

1516 83. Doret L, Poirel L, Abbas S, Oueslati S, Nordmann P. Genetic and biochemical
1517 characterization of FRI-1, a carbapenem-hydrolyzing class A β -lactamase from *Enterobacter*
1518 *cloacae*. *Antimicrob. Agents Chemother.* 2015;59(12):7420-5.

1519 84. Palzkill T. Metallo- β -lactamase structure and function. *Ann. N. Y. Acad. Sci.*
1520 2013;1277:91-104.

1521 85. Papp-Wallace KM, Bethel CR, Distler AM, Kasuboski C, Taracila M, Bonomo RA.
1522 Inhibitor resistance in the KPC-2 β -lactamase, a preeminent property of this class A beta-
1523 lactamase. *Antimicrob. Agents Chemother.* 2010;54(2):890-7.

1524 86. Zhang H, Srinivas S, Xu Y, Wei W, Feng Y. Genetic and biochemical mechanisms for
1525 bacterial lipid A modifiers associated with polymyxin resistance. *Trends Biochem. Sci.*
1526 2019;44(11):973-88.

1527 87. Corkill JE, Cuevas LE, Gurgel RQ, Greensill J, Hart CA. SHV-27, a novel
1528 cefotaxime-hydrolysing β -lactamase, identified in *Klebsiella pneumoniae* isolates from a
1529 Brazilian hospital. *J. Antimicrob. Chemother.* 2001;47(4):463-5.

1530 88. Silvestro L, Weiser JN, Axelsen PH. Antibacterial and antimembrane activities of
1531 cecropin A in *Escherichia coli*. *Antimicrob. Agents Chemother.* 2000;44(3):602-7.

1532 89. Casadaban MJ, Cohen SN. Analysis of gene control signals by DNA fusion and
1533 cloning in *Escherichia coli*. *J. Mol. Biol.* 1980;138(2):179-207.

1534 90. Hanahan D. In: Glover DM, editor. *DNA Cloning: A Practical Approach*. 1: IRL
1535 Press, McLean, Virginia; 1985. p. 109.

1536 91. Herrero M, de Lorenzo V, Timmis KN. Transposon vectors containing non-antibiotic
1537 resistance selection markers for cloning and stable chromosomal insertion of foreign genes in
1538 Gram-negative bacteria. *J. Bacteriol.* 1990;172(11):6557-67.

1539 92. Boyer HW, Roulland-Dussoix D. A complementation analysis of the restriction and
1540 modification of DNA in *Escherichia coli*. *J. Mol. Biol.* 1969;41(3):459-72.

1541 93. Blattner FR, Plunkett G, 3rd, Bloch CA, Perna NT, Burland V, Riley M, et al. The
1542 complete genome sequence of *Escherichia coli* K-12. *Science.* 1997;277(5331):1453-62.

1543 94. Doret L, Brechard L, Poirel L, Nordmann P. Rapid detection of carbapenemase-
1544 producing *Enterobacteriaceae* from blood cultures. *Clin. Microbiol. Infect.* 2014;20(4):340-
1545 4.

1546 95. Beyrouty R, Robin F, Lessene A, Lacombat I, Doret L, Naas T, et al. MCR-1 and
1547 OXA-48 *in vivo* acquisition in KPC-producing *Escherichia coli* after colistin treatment.
1548 *Antimicrob. Agents Chemother.* 2017;61(8).

1549 96. Haenni M, Beyrouty R, Lupo A, Chatre P, Madec JY, Bonnet R. Epidemic spread of
1550 *Escherichia coli* ST744 isolates carrying *mcr-3* and *blaCTX-M-55* in cattle in France. *J.*
1551 *Antimicrob. Chemother.* 2018;73(2):533-6.

1552 97. Wise MG, Estabrook MA, Sahm DF, Stone GG, Kazmierczak KM. Prevalence of
1553 *mcr*-type genes among colistin-resistant *Enterobacteriaceae* collected in 2014-2016 as part of
1554 the INFORM global surveillance program. *PloS One.* 2018;13(4):e0195281.

1555 98. Nordmann P, Poirel L, Dortet L. Rapid detection of carbapenemase-producing
1556 *Enterobacteriaceae*. *Emerg. Infect. Dis.* 2012;18(9):1503-7.

1557 99. Datsenko KA, Wanner BL. One-step inactivation of chromosomal genes in
1558 *Escherichia coli* K-12 using PCR products. *Proc. Natl. Acad. Sci. U.S.A.* 2000;97(12):6640-
1559 5.

1560 100. Kessler B, Delorenzo V, Timmis KN. A general system to integrate *lacZ* fusions into
1561 the chromosomes of Gram-negative eubacteria: regulation of the *Pm* Promoter of the *TOL*
1562 plasmid studied with all controlling elements in monocopy. *Mol. Gen. Genet.* 1992;233(1-
1563 2):293-301.

KEY RESOURCES TABLE

Reagent type (species) or resource	Designation	Source or reference	Identifiers	Additional information
Genetic reagent (<i>Escherichia coli</i>)	DH5 α	(90)	F $^-$ <i>endA1 glnV44 thi-1 recA1 relA1 gyrA96 deoR nupG purB20</i> ϕ 80dlacZ Δ M15 Δ (<i>lacZYA-argF</i>)U169 <i>hsdR17(rK$^-$mK$^+$) λ^- <i>araD</i> Δ(<i>ara, leu</i>) Δ<i>lacZ74 phoA20</i></i>	-
Genetic reagent (<i>Escherichia coli</i>)	CC118 λ pir	(91)	<i>galK thi-1 rspE rpoB argE recA1</i> λ pir <i>supE44 hsdS20 recA13 ara-14 proA2</i>	-
Genetic reagent (<i>Escherichia coli</i>)	HB101	(92)	<i>lacY1 galK2 rpsL20 xyl-5 mtl-1</i>	-
Genetic reagent (<i>Escherichia coli</i>)	MC1000	(89)	<i>araD139</i> Δ (<i>ara, leu</i>)7697 Δ <i>lacX74</i> <i>galU galK strA</i>	-
Genetic reagent (<i>Escherichia coli</i>)	MC1000 <i>dsbA</i>	(21)	<i>dsbA::aphA</i> , Kan R	-
Genetic reagent (<i>Escherichia coli</i>)	MC1000 <i>dsbA</i> <i>attTn7::Ptac-dsbA</i>	This study	<i>dsbA::aphA attTn7::dsbA</i> , Kan R	-
Genetic reagent (<i>Escherichia coli</i>)	MG1655	(93)	K-12 F $^-$ λ^- <i>ilvG^- rfb-50 rph-1</i>	-
Genetic reagent (<i>Escherichia coli</i>)	MG1655 <i>dsbA</i>	This study	<i>dsbA::aphA</i> , Kan R	-
Genetic reagent (<i>Escherichia coli</i>)	MG1655 <i>dsbA</i> <i>attTn7::Ptac-dsbA</i>	This study	<i>dsbA::aphA attTn7::dsbA</i> , Kan R	-
Genetic reagent (<i>Escherichia coli</i>)	MG1655 <i>acrA</i>	This study	<i>acrA</i>	-
Genetic reagent (<i>Escherichia coli</i>)	MG1655 <i>tolC</i>	This study	<i>tolC</i>	-
Genetic reagent (<i>Escherichia coli</i>)	MG1655 <i>degP</i>	This study	<i>degP::strAB</i> , Str R	-
Genetic reagent (<i>Escherichia coli</i>)	MG1655 <i>marR</i>	This study	<i>marR::accC</i> , Gent R	-
Genetic reagent	MG1655 <i>dsbA marR</i>	This study	<i>dsbA::aphA marR::accC</i> , Kan R , Gent R	-

(<i>Escherichia coli</i>)				
Strain, strain background (<i>Escherichia coli</i>)	BM16	(94)	<i>bla</i> _{TEM-1b} <i>bla</i> _{KPC-2}	Human clinical strain
Strain, strain background (<i>Escherichia coli</i>)	LIL-1	(94)	<i>bla</i> _{TEM-1} <i>bla</i> _{OXA-9} <i>bla</i> _{KPC-2}	Human clinical strain
Strain, strain background (<i>Escherichia coli</i>)	CNR1790	(43)	<i>bla</i> _{TEM-15} <i>mcr-1</i>	Human clinical strain
Strain, strain background (<i>Escherichia coli</i>)	CNR20140385	(43)	<i>bla</i> _{OXA-48} <i>mcr-1</i>	Human clinical strain
Strain, strain background (<i>Escherichia coli</i>)	WI2 (ST1288)	(95)	<i>bla</i> _{OXA-48} <i>bla</i> _{KPC-28} <i>mcr-1</i>	Human clinical strain
Strain, strain background (<i>Escherichia coli</i>)	27841 (ST744)	(96)	<i>bla</i> _{CTX-M-55} <i>mcr-3.2</i>	Environmental strain from livestock
Strain, strain background (<i>Escherichia coli</i>)	1144230 (ST641)	(97)	<i>bla</i> _{CMY-2} <i>mcr-5</i>	Human clinical strain
Strain, strain background (<i>Klebsiella pneumoniae</i>)	ST234	(98)	<i>bla</i> _{SHV-27} <i>bla</i> _{KPC-2}	Human clinical strain
Strain, strain background (<i>Citrobacter freundii</i>)	BM19	(94)	<i>bla</i> _{KPC-2}	Human clinical strain
Strain, strain background (<i>Enterobacter cloacae</i>)	DUB	(83)	<i>bla</i> _{FRI-1}	Human clinical strain
Strain, strain background (<i>Pseudomonas aeruginosa</i>)	PA43417	(82)	<i>bla</i> _{OXA-198}	Human clinical strain
Genetic reagent (<i>Pseudomonas aeruginosa</i>)	PA43417	This study	<i>dsbA1</i> <i>bla</i> _{OXA-198}	Human clinical strain
Strain, strain background (<i>Pseudomonas aeruginosa</i>)	PAe191	(56)	<i>bla</i> _{OXA-19}	Human clinical strain
Genetic reagent (<i>Pseudomonas aeruginosa</i>)	PAe191	This study	<i>dsbA1</i> <i>bla</i> _{OXA-19}	Human clinical strain
Recombinant DNA reagent	pDM1 (plasmid)	Lab stock	GenBank MN128719	pDM1 vector, p15A <i>ori</i> , <i>Ptac</i> promoter, MCS, <i>Tet</i> ^R
Recombinant DNA reagent	pDM1- <i>bla</i> _{L2-1} (plasmid)	This study	-	<i>bla</i> _{L2-1} cloned into pDM1, <i>Tet</i> ^R

Recombinant DNA reagent	pDM1- <i>bla</i> _{GES-1} (plasmid)	This study	-	<i>bla</i> _{GES-1} cloned into pDM1, Tet ^R
Recombinant DNA reagent	pDM1- <i>bla</i> _{GES-2} (plasmid)	This study	-	<i>bla</i> _{GES-2} cloned into pDM1, Tet ^R
Recombinant DNA reagent	pDM1- <i>bla</i> _{GES-11} (plasmid)	This study	-	<i>bla</i> _{GES-11} cloned into pDM1, Tet ^R
Recombinant DNA reagent	pDM1- <i>bla</i> _{SHV-27} (plasmid)	This study	-	<i>bla</i> _{SHV-27} cloned into pDM1, Tet ^R
Recombinant DNA reagent	pDM1- <i>bla</i> _{OXA-4} (plasmid)	This study	-	<i>bla</i> _{OXA-4} cloned into pDM1, Tet ^R
Recombinant DNA reagent	pDM1- <i>bla</i> _{OXA-10} (plasmid)	This study	-	<i>bla</i> _{OXA-10} cloned into pDM1, Tet ^R
Recombinant DNA reagent	pDM1- <i>bla</i> _{OXA-198} (plasmid)	This study	-	<i>bla</i> _{OXA-198} cloned into pDM1, Tet ^R
Recombinant DNA reagent	pDM1- <i>bla</i> _{FRI-1} (plasmid)	This study	-	<i>bla</i> _{FRI-1} cloned into pDM1, Tet ^R
Recombinant DNA reagent	pDM1- <i>bla</i> _{L1-1} (plasmid)	This study	-	<i>bla</i> _{L1-1} cloned into pDM1, Tet ^R
Recombinant DNA reagent	pDM1- <i>bla</i> _{KPC-2} (plasmid)	This study	-	<i>bla</i> _{KPC-2} cloned into pDM1, Tet ^R
Recombinant DNA reagent	pDM1- <i>bla</i> _{KPC-3} (plasmid)	This study	-	<i>bla</i> _{KPC-3} cloned into pDM1, Tet ^R
Recombinant DNA reagent	pDM1- <i>bla</i> _{SMES-1} (plasmid)	This study	-	<i>bla</i> _{SMES-1} cloned into pDM1, Tet ^R
Recombinant DNA reagent	pDM1- <i>mcr-1</i> (plasmid)	This study	-	<i>mcr-1</i> cloned into pDM1, Tet ^R
Recombinant DNA reagent	pDM1- <i>mcr-3</i> (plasmid)	This study	-	<i>mcr-3</i> cloned into pDM1, Tet ^R
Recombinant DNA reagent	pDM1- <i>mcr-3.2</i> (plasmid)	This study	-	<i>mcr-3.2</i> cloned into pDM1, Tet ^R
Recombinant DNA reagent	pDM1- <i>mcr-4</i> (plasmid)	This study	-	<i>mcr-4</i> cloned into pDM1, Tet ^R
Recombinant DNA reagent	pDM1- <i>mcr-5</i> (plasmid)	This study	-	<i>mcr-5</i> cloned into pDM1, Tet ^R
Recombinant DNA reagent	pDM1- <i>mcr-8</i> (plasmid)	This study	-	<i>mcr-8</i> cloned into pDM1, Tet ^R
Recombinant DNA reagent	pDM1- <i>bla</i> _{L2-1} -StrepII (plasmid)	This study	-	<i>bla</i> _{L2-1} encoding L2-1 with a C-terminal StrepII tag cloned into pDM1, Tet ^R
Recombinant DNA reagent	pDM1- <i>bla</i> _{GES-1} -StrepII (plasmid)	This study	-	<i>bla</i> _{GES-1} encoding GES-1 with a C-terminal StrepII tag cloned into pDM1, Tet ^R
Recombinant DNA reagent	pDM1-StrepII- <i>bla</i> _{OXA-4} (plasmid)	This study	-	<i>bla</i> _{OXA-4} encoding OXA-4 with an N-terminal StrepII tag cloned into pDM1, Tet ^R
Recombinant DNA reagent	pDM1- <i>bla</i> _{OXA-10} -StrepII (plasmid)	This study	-	<i>bla</i> _{OXA-10} encoding OXA-10 with a C-terminal StrepII tag cloned into pDM1, Tet ^R
Recombinant DNA reagent	pDM1- <i>bla</i> _{OXA-198} -StrepII (plasmid)	This study	-	<i>bla</i> _{OXA-198} encoding OXA-198 with a C-terminal StrepII tag cloned into pDM1,

Recombinant DNA reagent	pDM1- <i>bla</i> _{FRI-1} -StrepII (plasmid)	This study	-	Tet ^R <i>bla</i> _{FRI-1} encoding FRI-1 with a C-terminal StrepII tag cloned into pDM1, Tet ^R
Recombinant DNA reagent	pDM1- <i>bla</i> _{L1-1} -StrepII (plasmid)	This study	-	<i>bla</i> _{L1-1} encoding L1-1 with a C-terminal StrepII tag cloned into pDM1, Tet ^R
Recombinant DNA reagent	pDM1- <i>bla</i> _{KPC-3} -StrepII (plasmid)	This study	-	<i>bla</i> _{KPC-3} encoding KPC-3 with a C-terminal StrepII tag cloned into pDM1, Tet ^R
Recombinant DNA reagent	pDM1- <i>mcr</i> -1-StrepII (plasmid)	This study	-	<i>bla</i> _{MCR-1} encoding MCR-1 with a C-terminal StrepII tag cloned into pDM1, Tet ^R
Recombinant DNA reagent	pDM1- <i>mcr</i> -3-StrepII (plasmid)	This study	-	<i>bla</i> _{MCR-3} encoding MCR-3 with a C-terminal StrepII tag cloned into pDM1, Tet ^R
Recombinant DNA reagent	pDM1- <i>mcr</i> -4-StrepII (plasmid)	This study	-	<i>bla</i> _{MCR-4} encoding MCR-4 with a C-terminal StrepII tag cloned into pDM1, Tet ^R
Recombinant DNA reagent	pDM1- <i>mcr</i> -5-StrepII (plasmid)	This study	-	<i>bla</i> _{MCR-5} encoding MCR-5 with a C-terminal StrepII tag cloned into pDM1, Tet ^R
Recombinant DNA reagent	pDM1- <i>mcr</i> -8-StrepII (plasmid)	This study	-	<i>bla</i> _{MCR-8} encoding MCR-8 with a C-terminal StrepII tag cloned into pDM1, Tet ^R
Recombinant DNA reagent	pGRG25 (plasmid)	(67)	-	Encodes a Tn7 transposon and <i>tnsABCD</i> under the control of <i>ParaB</i> , thermosensitive pSC101 <i>ori</i> , Amp ^R
Recombinant DNA reagent	pGRG25- <i>Ptac::dsbA</i> (plasmid)	This study	-	<i>Ptac::dsbA</i> fragment cloned within the Tn7 of pGRG25; when inserted into the chromosome and the plasmid cured, the strain expresses DsbA upon IPTG induction, Amp ^R
Recombinant DNA reagent	pSLTS (plasmid)	(66)	-	Thermosensitive pSC101 <i>ori</i> , <i>ParaB</i> for λ-

Recombinant DNA reagent	pUltraGFP-GM (plasmid)	(71)	-	Red, <i>PtetR</i> for I-SceI, Amp ^R Constitutive sfGFP expression from a strong Biofab promoter, p15A <i>ori</i> , (template for the <i>accC</i> cassette), Gent ^R
Recombinant DNA reagent	pKD4 (plasmid)	(99)	-	Conditional oriR γ <i>ori</i> , (template for the <i>aphA</i> cassette), Amp ^R
Recombinant DNA reagent	pCB112 (plasmid)	(72)	-	Inducible <i>lacZ</i> expression under the control of the P _{lac} promoter, pBR322 <i>ori</i> , Cam ^R
Recombinant DNA reagent	pKNG101 (plasmid)	(69)	-	Gene replacement suicide vector, <i>oriR6K</i> , <i>oriTRK2</i> , <i>sacB</i> , (template for the <i>strAB</i> cassette), Str ^R
Recombinant DNA reagent	pKNG101- <i>dsbA1</i> (plasmid)	This study	-	PCR fragment containing the regions upstream and downstream <i>P. aeruginosa</i> <i>dsbA1</i> cloned in pKNG101; when inserted into the chromosome the strain is a merodiploid for <i>dsbA1</i> mutant, Str ^R
Recombinant DNA reagent	pRK600 (plasmid)	(100)	-	Helper plasmid, ColE1 <i>ori</i> , <i>mobRK2</i> , <i>trRK2</i> , Cam ^R
Recombinant DNA reagent	pMA-T <i>mcr-3</i> (plasmid)	This study	-	GeneArt® cloning vector containing <i>mcr-3</i> , ColE1 <i>ori</i> , (template for <i>mcr-3</i>), Amp ^R
Recombinant DNA reagent	pMK-T <i>mcr-8</i> (plasmid)	This study	-	GeneArt® cloning vector containing <i>mcr-8</i> , ColE1 <i>ori</i> , (template for <i>mcr-8</i>), Kan ^R
Chemical compound, drug	Ampicillin	Melford	A40040-10.0	-
Chemical compound, drug	Piperacillin	Melford	P55100-1.0	-
Chemical compound, drug	Cefuroxime	Melford	C56300-1.0	-
Chemical compound, drug	Ceftazidime	Melford	C59200-5.0	-
Chemical compound, drug	Imipenem	Cambridge Bioscience	CAY16039-100 mg	-
Chemical compound, drug	Aztreonam	Cambridge Bioscience	CAY19784-100 mg	-
Chemical compound, drug	Kanamycin	Gibco	11815032	-

Chemical compound, drug	Gentamicin	VWR	A1492.0025	-
Chemical compound, drug	Streptomycin	ACROS Organics	AC612240500	-
Chemical compound, drug	Tetracycline	Duchefa Biochemie	T0150.0025	-
Chemical compound, drug	Colistin sulphate	Sigma	C4461-1G	-
Chemical compound, drug	Tazobactam	Sigma	T2820-10MG	-
Chemical compound, drug	Isopropyl β -D-1-thiogalactopyranoside (IPTG)	Melford	I56000-25.0	-
Chemical compound, drug	KOD Hotstart DNA Polymerase	Sigma	71086-3	-
Chemical compound, drug	Nitrocefin	Abcam	ab145625-25mg	-
Chemical compound, drug	1-N-phenylnaphthylamine (NPN)	Acros Organics	147160250	-
Chemical compound, drug	4-acetamido-4'-maleimidyl-stilbene-2,2'-disulfonic acid (AMS)	ThermoFisher Scientific	A485	-
Chemical compound, drug	4,5-dichloro-2-(2-chlorobenzyl)pyridazin-3-one	Enamine	EN300-173996	-
Commercial assay, kit	BugBuster Mastermix	Sigma	71456-3	-
Commercial assay, kit	Novex ECL HRP chemiluminescent substrate reagent kit	ThermoFisher Scientific	WP20005	-
Commercial assay, kit	SigmaFast BCIP/NBT tablets	Sigma	B5655-25TAB	-
Commercial assay, kit	Immobilon Crescendo chemiluminescent reagent	Sigma	WBLUR0100	-
Commercial assay, kit	ETEST - Amoxicillin	Biomerieux	412242	-
Commercial assay, kit	ETEST - Cefuroxime	Biomerieux	412304	-
Commercial assay, kit	ETEST - Ceftazidime	Biomerieux	412292	-

Commercial assay, kit	ETEST - Imipenem	Biomerieux	412373	-
Commercial assay, kit	ETEST - Aztreonam	Biomerieux	412258	-
Commercial assay, kit	ETEST - Gentamicin	Biomerieux	412367	-
Commercial assay, kit	ETEST - Erythromycin	Biomerieux	412333	-
Commercial assay, kit	ETEST - Chloramphenicol	Biomerieux	412308	-
Commercial assay, kit	ETEST - Nalidixic acid	Biomerieux	516540	-
Commercial assay, kit	ETEST - Ciprofloxacin	Biomerieux	412310	-
Commercial assay, kit	ETEST - Nitrofurantoin	Biomerieux	530440	-
Commercial assay, kit	ETEST - Trimethoprim	Biomerieux	412482	-
Antibody	Strep-Tactin-HRP conjugate (mouse monoclonal)	Iba Lifesciences	NC9523094	1:3,000 in 3 w/v % BSA/TBS-T
Antibody	Strep-Tactin-AP conjugate (mouse monoclonal)	Iba Lifesciences	NC0485490	1:3,000 in 3 w/v % BSA/TBS-T
Antibody	anti-DsbA (rabbit polyclonal)	Beckwith lab	-	1:1,000 in 5 w/v % skimmed milk/TBS-T
Antibody	anti-AcrA (rabbit polyclonal)	Koronakis lab	-	1:10,000 in 5 w/v % skimmed milk/TBS-T
Antibody	anti-TolC (rabbit polyclonal)	Koronakis lab	-	1:5,000 in 5 w/v % skimmed milk/TBS-T
Antibody	anti-HtrA1 (DegP) (rabbit polyclonal)	Abcam	ab231195	1:1,000 in 5 w/v % skimmed milk/TBS-T
Antibody	anti-DnaK 8E2/2 (mouse monoclonal)	Enzo Life Sciences	ADI-SPA-880-D	1:10,000 in 5% w/v skimmed milk/TBS-T
Antibody	anti-rabbit IgG-AP conjugate (goat polyclonal)	Sigma	A3687-.25ML	1:6,000 in 5% w/v skimmed milk/TBS-T
Antibody	anti-rabbit IgG-HRP conjugate (goat polyclonal)	Sigma	A0545-1ML	1:6,000 in 5% w/v skimmed milk/TBS-T
Antibody	anti-mouse IgG-AP conjugate (goat	Sigma	A3688-.25ML	1:6,000 in 5% w/v skimmed milk/TBS-T

Antibody	polyclonal) anti-mouse IgG-HRP conjugate (goat polyclonal)	Sigma	A4416-.5ML	1:6,000 in 5% w/v skimmed milk/TBS-T
Software, algorithm	FlowJo	Tree Star	-	version 10.0.6
Software, algorithm	Adobe Photoshop CS4	Adobe	-	extended version 11.0
Software, algorithm	Prism	GraphPad	-	version 8.0.2
Software, algorithm	blastp	(77)	-	version 2.2.28+
Software, algorithm	USEARCH	(76)	-	version 7.0
Software, algorithm	MUSCLE	(78)	-	-
Software, algorithm	FastTree	(79)	-	version 2.1.7
Software, algorithm	HMMER	(80)	-	version 3.1b2